A thesis for the Degree of Doctor of Philosophy

Evaluation of anticancer potentials of physciosporin, a lichen-originated compound, in colorectal and breast cancer

İsa Taş

Department of Science and Information

The Graduate School

Sunchon National University

August, 2020

Evaluation of anticancer potentials of physciosporin, a lichen-originated compound, in colorectal and breast cancer

Supervised by Prof. Jae-Seoun, Hur
Co-supervised by Prof. Hangun Kim

Presented as thesis for the Degree of Doctor of Philosophy

İsa Taş

Department of Science and Information

The Graduate School

Sunchon National University

August, 2020

Approved as a qualified thesis of İsa Taş

For the Degree of Doctor of Philosophy

Approved by:

Chairman: Kyung Keun Min

Member: Hyung Ho Ha

Member: Man-Jeong Park

Member: Hangun Kim

Member: Jae-seoun Hur

The Graduate School of Sunchon National University

2020.08.

CONTENTS

LIST OF FIGURES

LIST OF TABLES

LIST OF ABBREVIATIONS

2-DG, 2-deoxy-d-glucose

AA, Antimycin A

ARP2, actin-related protein 2

ARP3, actin-related protein 3

BAX, BCL2 associated X, apoptosis regulator

BC, Breast cancer

BCA, Bicinchoninic acid

Bcl-XL, Bcl2-like 1

c-FOS, Fos proto-oncogene, AP-1 like

c-Jun, Transcription factor AP-1-like

c-Myc, Transcriptional regulator Myc-like

CAPN2, calpain 2

CDC42, cell division cycle 42

CCND1, Cyclin D1

CRC, Colorectal cancer

DMEM, Dulbecco's Modified Eagle Medium

DMSO, Dimethylsulfoxide

ECAR, Extracellular acidification rate

EMT, Epithelial-mesenchymal transition

FCCP, carbonyl cyanide 4-(trifluoromethoxy) phenylhydrazone

FITC, Fluorescein isothiocyanate

FOBI, Fluorescence-labeled organism bioimaging instrument

GAPDH, Glyceraldehyde-3-phosphate dehydrogenase

Glut1, Glucose transporter 1

HIF-1α, Hypoxia inducible factor 1 subunit alpha

iRFP, Near-infrared fluorescent protein

KITENIN, KAI1 C-terminal-interacting tetraspanin

LC-MS, Liquid chromatography–mass spectrometry

LDHA, Lactate dehydrogenase A

MTT, Methyl thiazolyl tetrazolium

NF-kB, nuclear factor kappa B subunit 1

OCR, Oxygen consumption rate

OXPHOS, Oxidative phosporylation

PARP, Poly-(ADP-ribose) polymerase

PBS, Phosphate-buffered saline

PFN1, Profilin 1

PHY, Physciosporin

PI, Propidium Iodide

PIK3CA, Phosphatidylinositol-4,5-bisphosphate 3-kinase catalytic subunit alpha

PKM2, Pyruvate kinase M1/2

RAC1, Rac family small GTPase 1

Rot, Rotenone

RPMI, Roswell Park Memorial Institute

STAT3, Signal transducer and activator of transcription 3

TLC, Thin-layer chromatography

qRT-PCR, Quantitative Real-Time PCR

VEGFA, Vascular endothelial growth factor A

VCL, Vinculin

WASF1, WAS protein family, member 1

WASF2, WAS protein family, member 2

ABSTRACT

Evaluation of anticancer potentials of physciosporin, a lichen-originated compound, in colorectal and breast cancer

İsa Taş

Department of Science and Information

The Graduate School

Sunchon National University

Supervised by Prof. Jae-Seoun Hur

Co-supervised by Hangun Kim

Lichens, which represent symbiotic associations of fungi and algae, are potential sources of numerous natural products. Physciosporin (PHY) is a potent secondary metabolite found in lichens and was recently reported to inhibit the motility of lung cancer cells via novel mechanisms. The present study investigated the anticancer potential of PHY on colorectal and breast cancer cells. PHY was isolated from lichen extract by preparative TLC. The effect of PHY on cell viability, motility and tumorigenicity was elucidated by MTT assay, hoechst staining, flow cytometric analysis, transwell invasion and migration assay, soft agar colony formation assay, Western blotting, qRT-PCR and PCR array *in vitro* as well as

tumorigenicity study *in vivo*. In the first chapter, PHY decreased the viability of various colorectal cancer (CRC) cell lines (Caco2, CT26, DLD1, HCT116 and SW620). Moreover, PHY elicited cytotoxic effects by inducing apoptosis at toxic concentrations. At non-toxic concentrations, PHY dose-dependently suppressed the invasion, migration, and colony formation of CRC cells. PHY inhibited the motility of CRC cells by suppressing epithelial-mesenchymal transition and downregulating actin-based motility markers. In addition, PHY downregulated β-catenin and its downstream target genes cyclin-D1 and c-Myc. Moreover, PHY modulated KAI1 C-terminal-interacting tetraspanin and KAI1 expression and downregulated the downstream transcription factors c-jun and c-fos. Finally, PHY administration showed considerable bioavailability and effectively decreased the growth of CRC xenografts in mice without causing toxicity. Therefore, PHY suppresses the growth and motility of CRC cells via novel mechanisms.

In the second chapter, effect of PHY was evaluated on breast cancer (BC) cells. we investigated the effects of PHY on growth, and metabolism of BC cells MCF-7 and MDA-MB-231. Our results indicated that PHY markedly inhibits BC cell growth. Cell cycle analysis and Annexin V-FITC/PI double staining showed that the toxic concentration of PHY induced the apoptosis on BC cells through the mitochondrial apoptotic pathway via the regulation of Bcl-2 family proteins BAX and Bcl-xL. In non-toxic concentration, PHY potently decreased the ability of migration, proliferation, and tumorigenesis in BC cells. Metabolic investigation

revealed that PHY treatment significantly diminished the bioenergetic profile by reducing the glucose uptake, ATP generation, and lactate production. Moreover, PHY alters glucose metabolism-related gene expressions such as Glut1 and PKM2 and downregulated transcription factors and oncogenes related with PKM2 including β-catenin, c-Myc, HIF-1α, NF-κB and STAT3. Orthotopic implantation mouse model of BC further confirmed that PHY treatment suppressed BC growth.

In conclusion, present results indicated that PHY possessed significant anticancer activity against BC and CRC cell lines in vitro. Furthermore, PHY inhibited tumor growth in orthotopic and skin xenograft mouse models, respectively. Together, these findings suggest that PHY has a potential further in vivo application as an anti-proliferative, anti-glycolytic and anti-tumorigenic agent.

Chapter I. Physciosporin suppresses the proliferation, motility, and tumorigenesis of colorectal cancer cells

1. Physciosporin suppresses the proliferation, motility and tumorigenesis of colorectal cancer cells

1.1. Introduction

Colorectal cancer (CRC) is the third most commonly diagnosed malignancy in men (10%) after lung and prostate cancers and is the second most commonly diagnosed malignancy in women (9.2%) after breast cancer worldwide (Redondo-Blanco et al., 2017). CRC is the fourth leading cause of cancer-related death worldwide, accounting for ~1.4 million new cases and almost 700,000 deaths in 2012 (Arnold et al., 2017). Although potential treatments, including surgery, chemotherapy, and molecular targeting therapies, have improved patient outcomes, the clinical prognosis of CRC patients remains inadequate (Zhai et al., 2017). Consequently, new and more effective treatments urgently need to be developed (Redondo-Blanco et al., 2017).

Lichens are symbiotic associations of fungi and photosynthetic partners (algae and cyanobacteria). They synthesise a wide range of secondary metabolites to defend against biotic and abiotic stresses (Nash, 2008). Lichens have been used for centuries as traditional medicines to treat wounds, skin disorders and respiratory/digestive problems (Crawford, 2015). Moreover, lichens have gained great attention as potential sources of therapeutic agents to treat numerous diseases, including cancer.

Physciosporin (PHY) is a depsidone-derived lichen metabolite found in several species belonging to the genus Pseudocyphellaria (Huneck and Yoshimura, 1996). We previously demonstrated that PHY elicits anti-metastatic effects on lung cancer cells and elucidated the underlying molecular mechanism (Yang et al., 2015). The current study aimed to investigate the effects of PHY on apoptosis, motility and tumorigenesis of CRC cells and to elucidate the underlying molecular mechanisms.

1.2. Materials and Methods

1.2.1. Isolation and identification of PHY

Physciosporin (PHY) was detected in acetone extract of Chilean lichen *Pseudocyphellaria granulata* (CL130259) by HPLC analysis (Figure 1.1). Isolation of PHY was carried out by preparative thin-layer chromatography (TLC) method. The extracts were dissolved in 1 ml dichloromethane for 3 min in 1.5 ml Eppendorf tubes and then dropped onto Silica gel 60 F_{254}-precoated plates (Merck Millipore, Darmstadt, Germany) by a capillary tube. The constituents of the extract were eluted using 5% methanol/dichloromethane. A TLC plate was placed into the running chamber with elution solvent and removed when the solvent reached the final 2 cm of plate. A PHY standard was used as a control to identify the PHY spot among all the eluted compounds. The identified spot was scratched off and washed with 10% methanol/dichloromethane for 20 min. After filtration, the supernatant was evaporated using nitrogen gas and weighed. Liquid chromatography-mass spectrometry (LC-MS, Agilent Technologies, Santa Clara, CA, USA) was performed to confirm single peak within the purified sample. It was detected that the purity of isolated PHY is % 99.15 (Figure 1.2). Moreover, structure of PHY was confirmed by nuclear magnetic resonance (NMR, JOEL, Ltd., Tokyo, Japan) analysis (Figure 1.3).

Figure 1.1. HPLC analysis of acetone extract of *Pseudocyphellaria granulata* (CL130259)

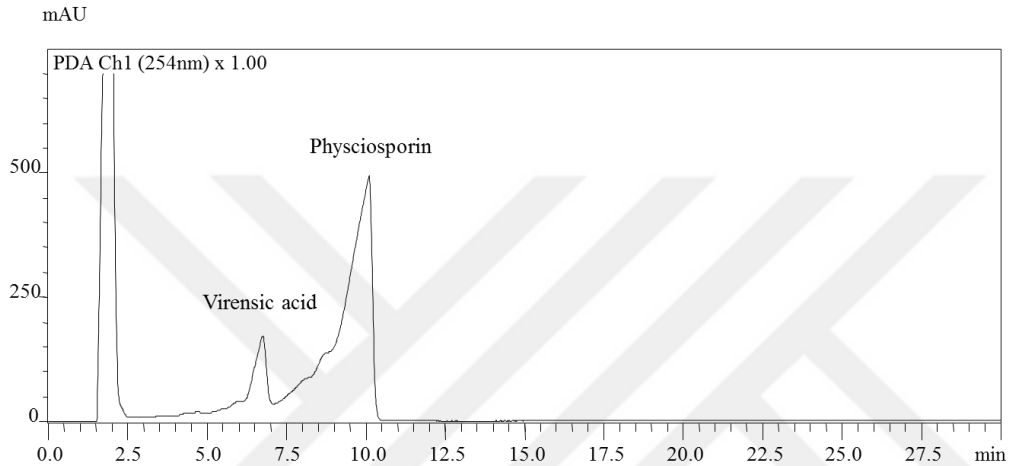

Figure 1.2. LC-MS analysis of PHY

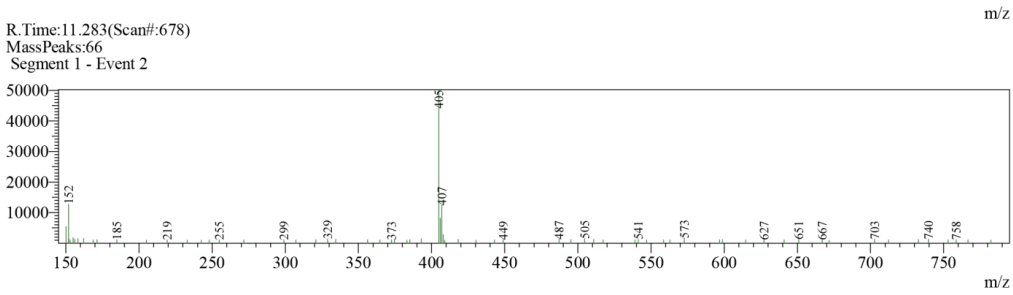

Peak Table

Detector A 254nm

Peak#	Ret. Time	Area	Height	Conc.	Unit	Mark	Name
1	2.314	31707	5872	0.849			
2	11.253	3702217	392037	99.151			
Total		3733924	397908				

Figure 1.3. ^{1}H-NMR data of PHY

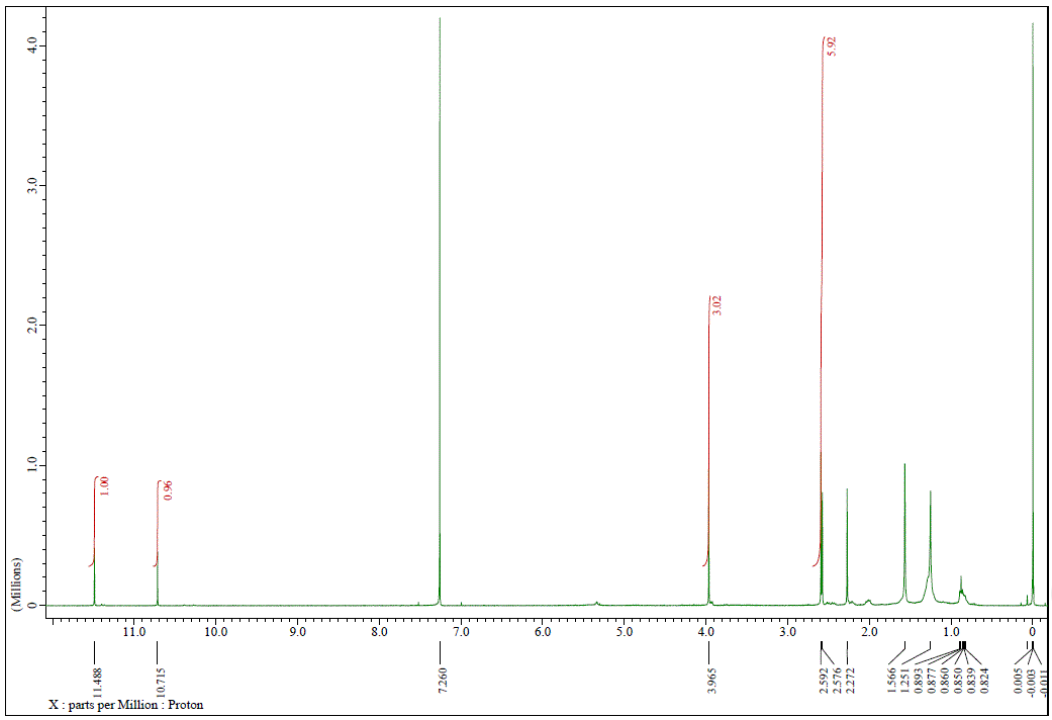

1.2.2. Cell culture

Caco2, DLD1, HCT116 and SW620 human CRC cells, CT26 mouse CRC cells and Madin-Darby canine kidney (MDCK) cells were used. All cells were cultured in Dulbecco's Modified Eagle Medium (DMEM) (Gen Depot, Katy, TX, USA) supplemented with 10% foetal bovine serum and 1% penicillin-streptomycin solution in a humidified atmosphere containing 5% CO2 at 37°C.

1.2.3. Methyl thiazolyl tetrazolium (MTT) assay

PHY was dissolved in dimethyl sulfoxide (DMSO; Sigma-Aldrich, St. Louis, MO, USA) and diluted to four concentrations (3, 6, 10 and 30 μg/mL). Cells were seeded into 96-well plates at a density of 1.5×10^3 cells/well (CT26), 2×10^3 cells/well (Caco2 and SW620) or 2.5×10^3 cells/well (DLD1 and HCT116), incubated overnight, and treated with DMSO or the indicated concentrations of PHY for 48 h. Next, 15 μL MTT (Sigma-Aldrich) was added and cells were incubated for an additional 4 h. Thereafter, the culture medium was carefully removed, and formazan crystals were dissolved in 150 μL DMSO. Absorbance at 570 nm was measured using a microplate reader and Gen 5 (2.03.1) software (BioTek, Winooski, VT, USA). The percentage of viable cells was calculated using the following formula:

$$\frac{\text{Optical density of the treated sample} \times 100}{\text{Optical density of the control sample}}$$

Usnic acid was used as a positive control. IC_{50} values were calculated using Statistical Package for Social Science software.

1.2.4. Invasion assay

Cell invasion was assessed using Boyden chambers (Corning, New York, NY, USA) coated with 1% gelatin. A total of 1×10^5 CRC cells in 100 μL DMEM containing 0.2% bovine serum albumin (BSA) were plated onto precoated inserts and incubated with 0.4, 0.8 or 1.6 μg/mL PHY or DMSO for 24 h. The lower chamber was filled with 600 μL DMEM containing 0.2% BSA and 10 μg/mL fibronectin (EMD Millipore Corp., Billerica, MA, USA) as a chemoattractant. After incubation, cells in the upper chamber were fixed and stained using a Diff-Quick kit (Sysmex, Kobe, Japan). The numbers of cells in five fields per chamber were counted using a Nikon Eclipse 400 fluorescence microscope (Nikon Instech, Co., Ltd, Kawasaki, Japan) and iSolution FL Autosoftware (IMT i-solution Inc., Vancouver, Quebec, Canada).

1.2.5. Migration assay

Cell migration was assessed using non-coated Boyden chambers. A total of 1×10^5 CRC cells were resuspended in 100 μL DMEM containing 0.2% BSA. The lower chamber was filled with 600 μL DMEM containing 0.2% BSA and fibronectin as a chemoattractant together with DMSO or 0.4, 0.8 or 1.6 μg/mL PHY. After incubation at 37°C for 24 h, migrated cells were fixed and stained using a Diff-Quick kit. The numbers of cells in five fields per chamber were counted using a Nikon Eclipse 400 fluorescence microscope (Nikon Instech, Co., Ltd.) and iSolution FL Autosoftware (IMT i-solution Inc.)

1.2.6. Soft agar colony formation assay

A total of 2.5×10^3 CRC cells were suspended in 1 mL of 0.35% upper layer (agarose diluted 2-fold with 2× DMEM) and overlaid onto 1 mL of 0.5% base layer (agarose diluted 2-fold with 2× DMEM) in a 12-well plate and cultured for 3 weeks. Feeder medium (culture medium containing the indicated concentrations of PHY or DMSO) was refreshed every 3 days. The surface areas of colonies in five fields per well were counted using a Nikon Eclipse 400 fluorescence microscope (Nikon Instech, Co., Ltd.) and iSolution FL Autosoftware (IMT i-solution Inc.) Three replicates were performed.

1.2.7. Hoechst staining

CRC cells were treated with PHY for 24 h in a 12-well plate, washed with phosphate-buffered saline (PBS), fixed in 4% paraformaldehyde for 15 min, permeabilised in 0.1% Triton X-100 (Sigma-Aldrich) for 30 min and incubated with Hoechst 33257 (Sigma-Aldrich) for 30 min at room temperature. Stained cells were mounted onto glass coverslips and analysed using a Nikon Eclipse 400 fluorescence microscope (Nikon Instech Co., Ltd) and iSolution FL Autosoftware (IMT i-solution Inc.).

1.2.8. Flow cytometric analysis

CRC cells were seeded into a 6-well plate at a density of 1×10^5 cells/well, cultured overnight, treated with toxic concentrations (16 and 24 µg/mL) of PHY for 48 h, trypsinized, washed with cold PBS and centrifuged at 1200 rpm for 5 min. To analyse the apoptotic population, cells were resuspended in 1× Binding Buffer and incubated with 2.5 µL Annexin-V-FITC and 5 µL propidium iodide (PI) on ice for 15 min in the dark. Stained cells were analysed using a Cytoflex flow cytometer (Beckman Coulter Life Sciences, Indianapolis, IN, USA) and CytExpert 2.0.0.152 software.

1.2.9. Quantitative real-time PCR

Total RNA was isolated from CRC cells using RNAiso Plus (TaKaRa, Otsu, Japan) according to the manufacturer's instructions. A total of 1 μg RNA was converted into cDNA using M-MLV reverse transcriptase (Invitrogen, Carlsbad, CA, USA). Relative gene expression was analysed using SYBR Green (Enzynomics, Seoul, Korea). The primers used for real-time PCR are listed in the Table 1. Real-time PCR was performed, and data were analysed using CFX (Bio-Rad, Hercules, CA, USA).

Table 1. The primers used for qRT-PCR.

Gene Symbol	Primers sequences		Accession	Product Length (bp)
	For (5'-3')	Rev (5'-3')		
ARP2	CCACCTAGTGTGCTAAAGACTACG	TCAACTCCAGGACATGGAAG	NM_005722.3	271
ARP3	TAATAAAAGCAAAGTGCAGAAC	TTCAAACAGTACCCAAAGAGTAG	NM_005721.4	204
CAPN2	CCAGAGGAGTTAAGTGGGCA	AGAAAAGACCCGGATGCAGA	NM_001146068.1	201
Vinculin	GCACCCAGCTCAAAAATCCTG	TCAGCCAGGTGCCTACTGGT	NM_003373.3	239
CDC42	TAAGTGTGTTGTTGTGGGCG	TCAGCGGTCGTAATCTGTCA	NM_001791.3	200
PIK3CA	CCACGACCATCATCAGGTGAA	CCTCACGGAGGCATTCTAAAGT	NM_006218.3	112
PFN1	GAACGCCTACATCGACAACC	AAACTTGACCGGTCTTTGCC	NM_005022.3	165
RAC1	CATCAAGTGTGTGGTGGTGG	TAAGCCCAGATTCACCGGTT	NM_006908.4	157
VEGFA	GGCCAGCACATAGGAGAGAT	ACGCTCCAGGACTTATACCG	NM_001025366.2	155
WASF1	AGTTCTTCACCCAGCTCCTC	GGTGATGATGGTCGAATGCC	NM_003931.2	186
WASF2	GAAACTCTCTCCCAGTGCCT	TGCAGCATCTTCTCCTTCCA	NM_006990.4	160
N-cadherin	CTCCTATGAGTGGAACAGGAACG	TTGGATCA ATGTCATAATCA AGTGCTGTA		
SNAIL	TCCCGGGCAATTTAACAATG	TGGGAGACACATCGGTCAGA	NM_005985.3	101
TWIST	CGGGAGTCCGCA GTCTTA	TGAATCTTGCTCAGCTTGTC	NM_000474.3	150
ZEB1	ATGACA CAGGAAAGGAAGG	AGCAGTGTCTTGTTGTAG	NM_001323657.1	158
ZEB2	CAAGAGGCGCAAACAAGCC	GGTTGGCAATACCGTCATCC	NM_014795.3	128
SLUG	CGAACTGGACACACATACAGTG	CTGAGGATC TCTGGTTGTGGT	NM_003068.4	87
KAI1	GCTCATGGGCTTGGGCT	GAGCTCAGTCACGATGCCGC		
KITENIN	CGGAATAAAGACGGCAGAGG	TGCTCCGAGGTGCCTGTGAT	NM_138959.2	152
Cyclin D1	CCGTCCATGCGGAAGATC	GAAGACCTCCTCCTCGCACT	NM_053056.2	75
C-MYC	AATGAAAAGGCCCCCAAGGTAGTT ATCC	GTCGTTTCCGCAACAAGTCCTCTTC	NM_002467.5	112
GAPDH	ATCACCATCTTC CAGGAGCGA	AGTTGTCATGGATGACCTTGGC	NM_002046.6	283

1.2.10. Western blotting

Cells were cultured in a 6-well plate for 12 h, treated with toxic (16 and 24 μg/mL) or non-toxic (0.4, 0.8 and 1.6 μg/mL) concentrations of PHY for 48 h, washed twice with cold PBS and lysed in lysis buffer. Whole cell extracts were prepared. In some experiments, nuclear and cytoplasmic fractions were isolated using NE-PER Nuclear and Cytoplasmic Extraction Reagents (Pierce, Rockford, IL, USA) according to the manufacturer's instructions. Protein concentrations were determined by the bicinchoninic acid protein assay (Thermo Fisher Scientific, Waltham, MA, USA). Membranes were probed with primary antibodies against β-catenin, poly (ADP-ribose) polymerase (PARP), caspase-3, c-Jun, Phospho-c-Jun, c-Fos and α-tubulin (Cell Signaling Technology, USA), E-cadherin and N-cadherin (BD Bioscience, USA), VANGL-1 (KITENIN) (Atlas Antibodies, Sweden), Snail/Slug and Twist (Abcam, UK), α-Histone H3 (Merck Millipore, Germany) and Zeb2 (Sigma-Aldrich, UK). Primary antibodies were detected with horseradish peroxidase-conjugated secondary antibodies (Thermo Fisher Scientific) using an Immobilon Western Chemiluminescent HRP Substrate Kit (Merck Millipore, Germany) and luminescence imaging (iBright™ FL1000 Imaging System, Thermo Fisher Sciences). The band densities were measured using Multi-Gauge 3.0 and normalised against that of α-tubulin or α-Histone H3 in each sample. Values are expressed as arbitrary densitometric units corresponding to the signal intensities.

1.2.11. Pathway-focused expression analysis using the RT2 profiler ^{TM} PCR array

The Human Cell Motility RT² Profiler™ PCR Array (Qiagen, SA Biosciences, Valencia, CA, USA) was used to assess expression of cell motility-related genes in PHY-treated cells. Expression of 84 key genes associated with cell motility was quantified according to the manufacturer's protocol. Fold changes in mRNA expression were calculated based on the cycle threshold values obtained by RT-PCR. A scatter plot of test versus control samples demonstrated the validity of the experiment.

1.2.12. Detection of PHY concentration in mice plasma

(Sample preparation for LC-MS/MS analysis) Stock solutions (10 mM) of PHY were prepared by dissolution in acetonitrile. Stock standard solutions were stored at -20°C. A working standard solution was prepared by dilution of the stock standard solution with a mixture of acetonitrile-water (1:1, v/v). The working standard solution was serially diluted to prepare a concentration series of 0.123, 0.37, 1.11, 3.33, and 10 μM in 50% acetonitrile.

PHY at 30 mg/kg was administered intraperitoneally, and plasma samples were collected after 24 h (n = 2 each). Plasma samples were prepared for analysis in a 96-well cluster tube plate by protein precipitation. A volume of 30 μL of each sample was transferred to eight-well tube strips placed in an 8 × 12 rack (VWR,

Emeryville, CA, USA). Four volumes of ice-cold extraction solution (acetonitrile) were added and vortexed for 10 min. After sonication for 30 min, samples were placed on ice for 1 h. The 96-well cluster tube plate was centrifuged at 1000 g for 10 min, and the supernatant was analyzed by LC-MS/MS. Standard samples were prepared in the same manner using a blank matrix.

(LC-MS/MS analysis) Samples were analyzed with the Prominence UPLC system (Shimadzu, Japan) equipped with an API 3200 QTRAP™ LC-MS/MS system (Applied Biosystems, Foster City, CA, USA). Sample volumes of 10 μL were injected into an atlantis dC18 column (2.1 × 50 mm, 3 μm i.d.; Waters, Milford, MA, USA) and maintained at 30°C. The column was pre-equilibrated in 80% v/v solvent A (deionized water containing 0.1% v/v formic acid)/20% v/v solvent B (acetonitrile containing 0.1% v/v formic acid) at a flow rate of 0.4 mL/min. The optimized LC elution conditions were 0.0–1.0 min, 20% B; 1.1–2.5 min, 95% B; 2.5–5.0 min, 95% B; 5.0–5.01 min, 20% B; and 5.01–6.0 min, 20% B. The overall chromatographic run time was 6 min. The autosampler compartment was maintained at 10°C throughout the analysis. The retention times of PHY was 3.49 min. The ESI source was operated at -4500 V and 600°C in a negative mode. Quadrupoles Q1 and Q3 were set on unity resolution. The samples were analyzed via multiple reaction monitoring. The monitoring ions was set as m/z 405→329 for

PHY. The acquisition and analysis of data were performed with Analyst™ software (version 1.5.2; Applied Biosystems).

1.2.13. In vivo tumorigenicity study

The anti-tumour activity of PHY was assessed using CRC xenografts. All animal experiments were approved by the Sunchon National University Research Institutional Animal Care & Use Committee. Male BALB/C mice (5-week-old) were purchased from OrientBio (Gyeonggi-do, Korea). After determination of treatment concentration, a total of 1×10^6 CT26 cells were implanted subcutaneously into the right flank of each mouse. When the tumour volume reached 100 mm^3, mice were intraperitoneally injected with vehicle (DMSO/PBS) or PHY at a dose of 7.5 mg/kg body weight once every 2 days. Calliper measurements were performed every 2 days. Tumour volumes were calculated using the following formula: volume in $mm^3 = 0.5 \times L \times W2$, where L is length and W is width. Tumours were monitored regularly and allowed to grow until the tumour volume in control mice reached ~1500 mm3. Thereafter, mice were sacrificed, and tumours were excised and weighed.

1.2.14. Statistical analysis

All in vitro experiments were performed in triplicate. Data are expressed as means ± standard error of results. The Student's t-test was utilized to determine statistical significance between two groups, and analysis of variance was utilized between three or more groups, respectively. P-values of <0.05 are considered statistically significant. All statistical analyses were performed using Statistical Package for Social Science and Sigma Plot software.

1.3. Results

1.3.1. PHY decreases the viability of CRC cells

PHY, a chlorinated depsidone, was isolated from *Pseudocyphellaria* sp. (CL130259) (Fig. 1.4A). We investigated whether treatment with various concentrations of PHY affected the viability of CRC cell lines (Caco2, CT26, DLD1, HCT116 and SW620) and a non-cancer cell line (MDCK) using the MTT assay. Treatment with 3–30 μg/mL PHY for 48 h dose-dependently decreased the viability of CRC cells (Fig. 1.4B and 1.4C). PHY most potently decreased the viability of CT26 (IC_{50}: 11.5 μg/mL), SW620 (IC_{50}: 12.6 μg/mL) and Caco2 (IC_{50}: 13.3 μg/mL) cells, while HCT116 and DLD1 cells were less affected by PHY (IC_{50}: 19.8 and 24.9 μg/mL, respectively). Moreover, PHY was lowly cytotoxic to MDCK cells (IC_{50}: 29.7 μg/mL = 73.02 μM). Usnic acid, used as positive control drug, showed less cytotoxicity to MDCK (IC_{50} = 45.8 μg/mL = 133.04 μM), and Caco2 (IC_{50} = 25.81 μg/mL) cells when compared with PHY. In summary, PHY has potent anti-proliferative effects on CRC cell lines.

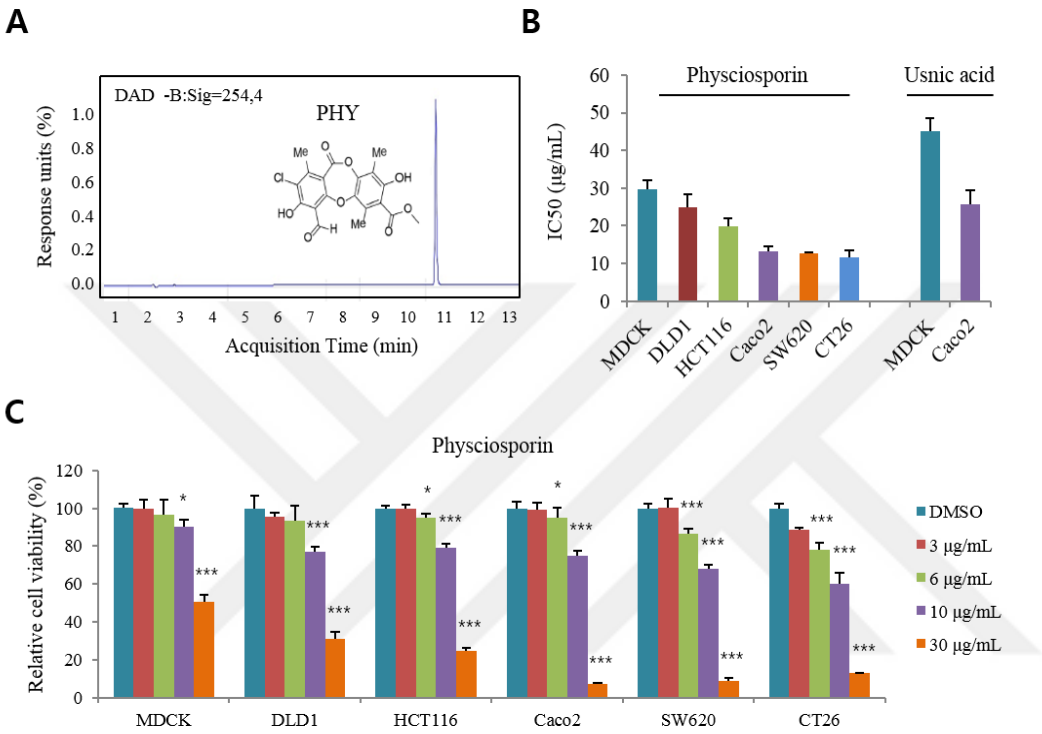

Figure 1.4. PHY decreases the viability of CRC cells in a dose-dependent manner. (A) Chemical structure and LC-MS data of PHY. (B) Non-cancer MDCK cells and five CRC cell lines (Caco2, CT26, DLD1, HCT116 and SW620) were seeded into 96-well plates, cultured for 12 h and treated with various concentrations (3, 6, 10 and 30 μg/mL) of PHY for 48 h. Cell viability was measured using the MTT assay, and IC_{50} values were calculated. Usnic acid was used as a positive control. (C) Relative viability of CRC and non-cancer cells upon PHY treatment. Data represent the mean ± standard error of the mean, n = 3. * $P < 0.05$; ** $P < 0.01$; *** $P < 0.001$.

1.3.2. PHY elicits cytotoxic effects on CRC cells by inducing apoptosis

Many chemical compounds inhibit the proliferation of cancer cells by triggering apoptosis (Hu et al., 2018). To determine whether the cytotoxic effect of PHY is due to the induction of apoptosis, we treated CRC cells with toxic concentrations (16 and 24 μg/mL) of PHY and performed Hoechst 33258 staining. This suggested that PHY induced nuclear condensation in CRC cells (Fig. 1.5A). The numbers of CRC cells with condensed nuclei were quantified (Fig. 1.5B). We performed flow cytometric analysis of samples co-stained with Annexin V-FITC and PI to determine the percentage of apoptotic cells. Treatment with toxic concentrations of PHY significantly increased the percentages of apoptotic cells (Fig. 1.5C and 1.5D). The percentages of apoptotic Caco2, HCT116 and SW620 cells following treatment with 24 μg/mL PHY were 58%, 62% and 62.9%, respectively (Fig. 1.5D). To confirm that PHY induces apoptosis of CRC cells, we investigated expression of the apoptosis-related proteins PARP and caspase-3 by western blotting. Activation of caspases induces apoptosis. Cleaved PARP is downstream of caspase-3 and is involved in several cellular processes, including DNA repair and apoptosis (Lee et al., 2014). PHY increased the levels of cleaved PARP and caspase-3 (Fig. 1.5E). Taken together, these results show that treatment with toxic concentrations of PHY reduces the viability of CRC cells by inducing apoptosis.

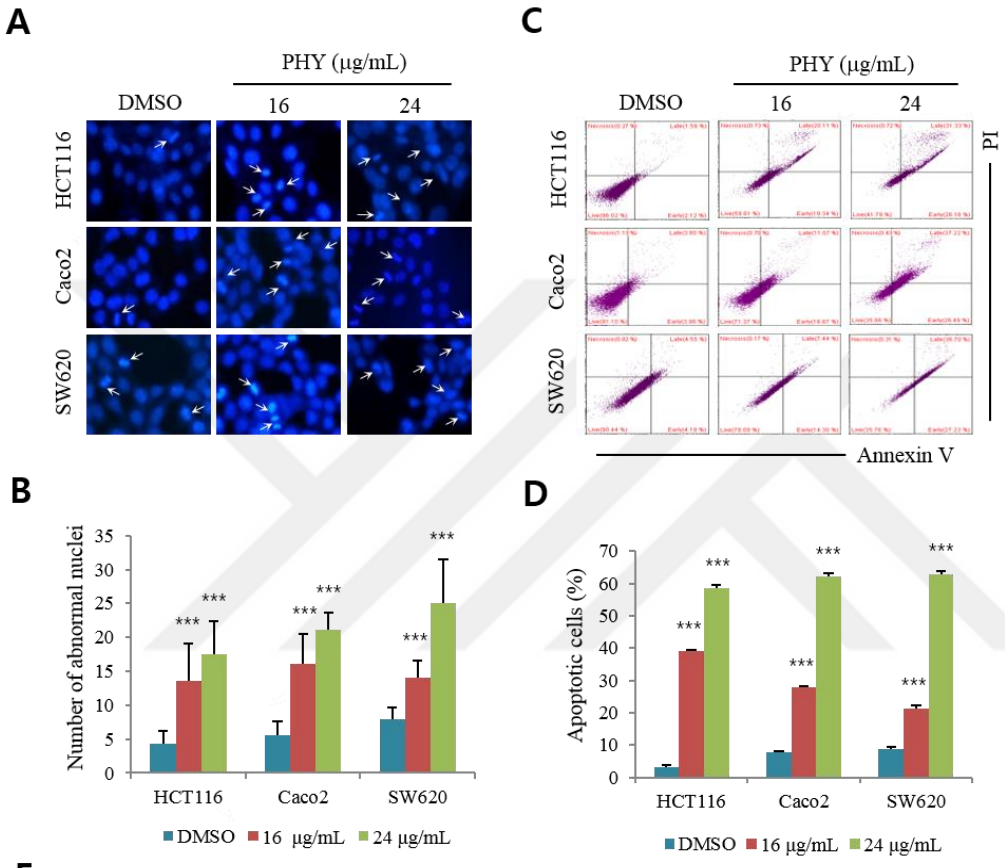
A
PHY (μg/mL)
DMSO
16
24
HCT116
Caco2
SW620
C
PHY (μg/mL)
DMSO
16
24
HCT116
Caco2
SW620
PI
Annexin V
B
Number of abnormal nuclei
35
30
25
20
15
10
5
0
***
HCT116
Caco2
SW620
DMSO
16 μg/mL
24 μg/mL
D
Apoptotic cells (%)
70
60
50
40
30
20
10
0
***
HCT116
Caco2
SW620
DMSO
16 μg/mL
24 μg/mL
E
HCT116
Caco2
SW620
PHY (μg/mL)
0
16
24
PARP
Caspase-3'
α-tubulin

Figure 1.5. Treatment with toxic concentrations of PHY induces apoptosis of CRC cells. CRC cells were cultured in the presence of toxic concentrations (16 and 24 μg/mL) of PHY for 48 h. (A) Fluorescence microscopy images of CRC cells stained with Hoechst 33258. Arrows indicate condensed nuclei. (B) Numbers of cells with condensed nuclei. (C) Samples were stained with Annexin V-FITC/PI to analyse apoptotic and necrotic cells and assessed using a Cytoflex flow cytometer. (D) Percentages of apoptotic cells. (E) Western blot analysis of the apoptosis-related proteins PARP and caspase-3 in PHY-treated cells. α-Tubulin served as a loading control. Data represent the mean ± standard error of the mean, n = 3. *** $P < 0.001$.

1.3.3. PHY suppresses the motility and tumorigenic potential of CRC cells

Tumour growth, migration and invasion are critical during cancer development and progression (Zhao et al., 2018). Tumour cells derived from the epithelium must be migratory and invasive to spread from primary tumours into the blood circulation (Yeung and Yang, 2017). Transwell assays were performed with and without gelatin coating to assess the effects of PHY on the invasion and migration of CRC cells, respectively. Cells were treated with non-toxic concentrations (0.4, 0.8 and 1.6 µg/mL) of PHY. PHY dose-dependently decreased the number of CRC cells that migrated (Fig. 1.6A and 1.6B). Moreover, PHY most affected the migration of Caco2 cells; treatment with 1.6 µg/mL PHY inhibited the migration of these cells by ~90%. In addition, PHY dose-dependently decreased the invasion of CRC cells. PHY most affected the invasion of HCT116 cells; treatment with 1.6 µg/mL PHY inhibited the invasion of these cells by ~70%. (Fig. 1.6C and 1.6D) A soft agar colony formation assay was performed to investigate the effect of PHY on the tumorigenic potential of CRC cells. PHY dose-dependently decreased colony formation by CRC cells (Fig. 1.6E and 1.6F). Caco2 cells were more sensitive to treatment with 1.6 µg/mL PHY than HCT116 and SW620 cells. Taken together, these results demonstrate that treatment with non-toxic concentrations of PHY significantly suppresses the motility and tumorigenicity of CRC cell lines.

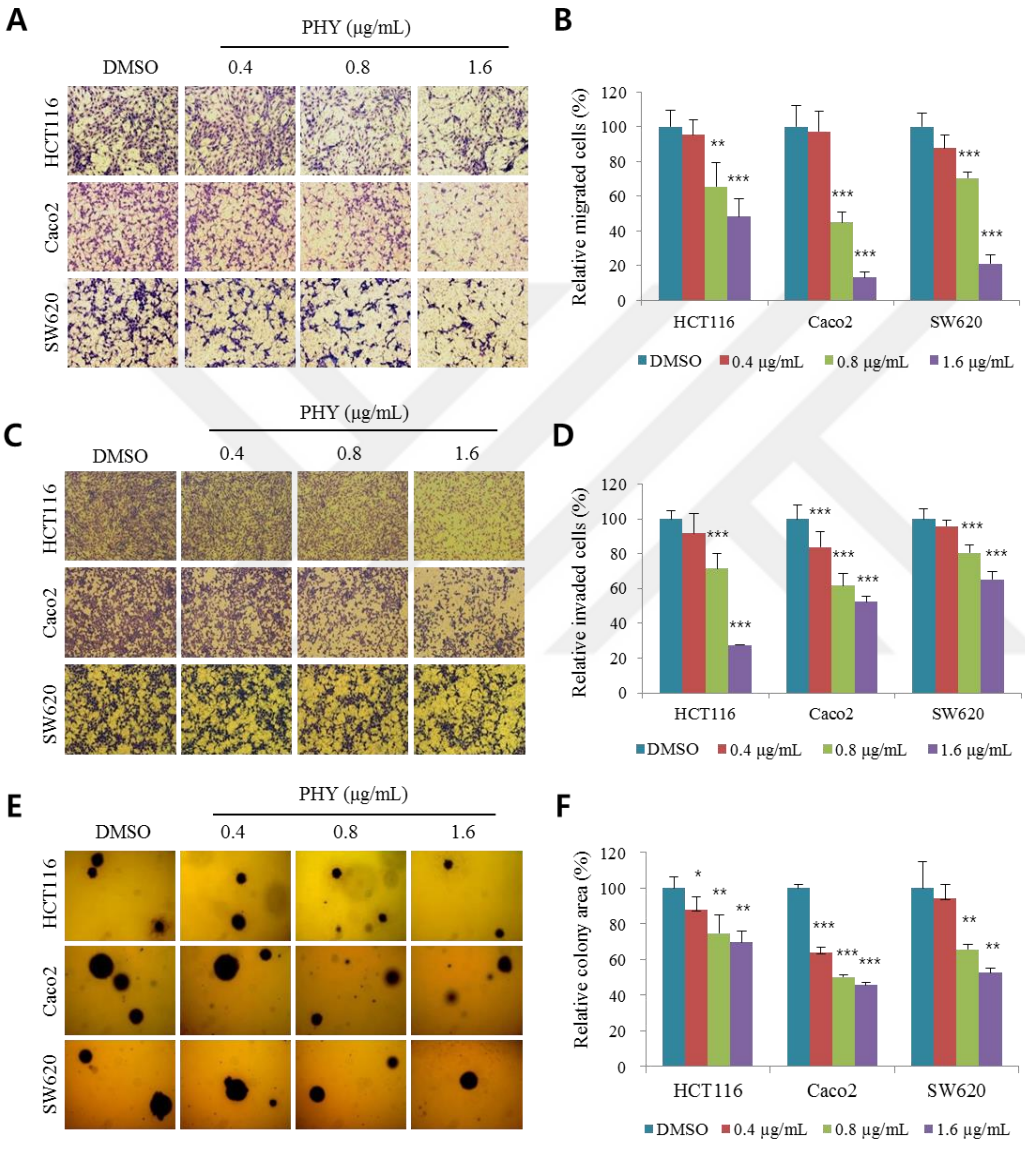
A
PHY (μg/mL)
DMSO
0.4
0.8
1.6
HCT116
Caco2
SW620
B
Relative migrated cells (%)
HCT116
Caco2
SW620
DMSO
0.4 μg/mL
0.8 μg/mL
1.6 μg/mL
C
D
Relative invaded cells (%)
E
F
Relative colony area (%)

Figure 1.6. Treatment with non-toxic concentrations of PHY significantly suppresses the motility and tumorigenicity of CRC cells. Transwell assays were performed with and without gelatin coating to assess the effects of PHY on the invasion and migration of CRC cells, respectively. Cells were treated with non-toxic concentrations (0.4, 0.8 and 1.6 μg/mL) of PHY for 24 h. (A) Representative images of each insert in the transwell migration assay. (B) Relative percentage of migrated cells. (C) Representative images of each insert in the transwell invasion assay. (D) Relative percentage of invaded cells. A soft agar colony formation assay was performed to assess the anti-tumorigenic potential of PHY. Cells were seeded into 12-well plates at a density of 2500 cells/well and treated with non-toxic concentrations of PHY for 2 weeks. The culture medium was refreshed every 3 days. (E) Representative images of colonies formed by PHY-treated cells. (F) Relative surface area of colonies. Data represent the mean ± standard error of the mean, n = 3. * $P < 0.05$; ** $P < 0.01$; *** $P < 0.001$.

1.3.4. PHY modulates expression of epithelial-mesenchymal transition (EMT) effectors and downregulates EMT transcription factors

EMT facilitates invasion and dissemination of tumour cells to distant organs and is thereby a key regulator of metastasis (Santamaria et al., 2017) (Fig. 1.7A). Expression of several EMT markers was analysed to determine whether PHY suppresses the invasion and migration of CRC cells by modulating EMT. PHY dose-dependently decreased mRNA expression of the mesenchymal markers vimentin and N-cadherin, but did not significantly affect that of the epithelial marker E-cadherin (Fig. 1.7B). Moreover, PHY significantly decreased mRNA expression of the EMT transcription factors Snail, Slug, Twist, Zeb1 and Zeb2 (Fig. 1.7C). These results were confirmed by analysis of the effects of PHY on protein expression of E-cadherin, N-cadherin, Snail and Zeb2 (Fig. 1.7D and 1.7E). In summary, these results indicate that PHY modulates expression of the EMT effectors N-cadherin and vimentin by downregulating the transcription factors Snail, Slug, Twist, Zeb1 and Zeb2.

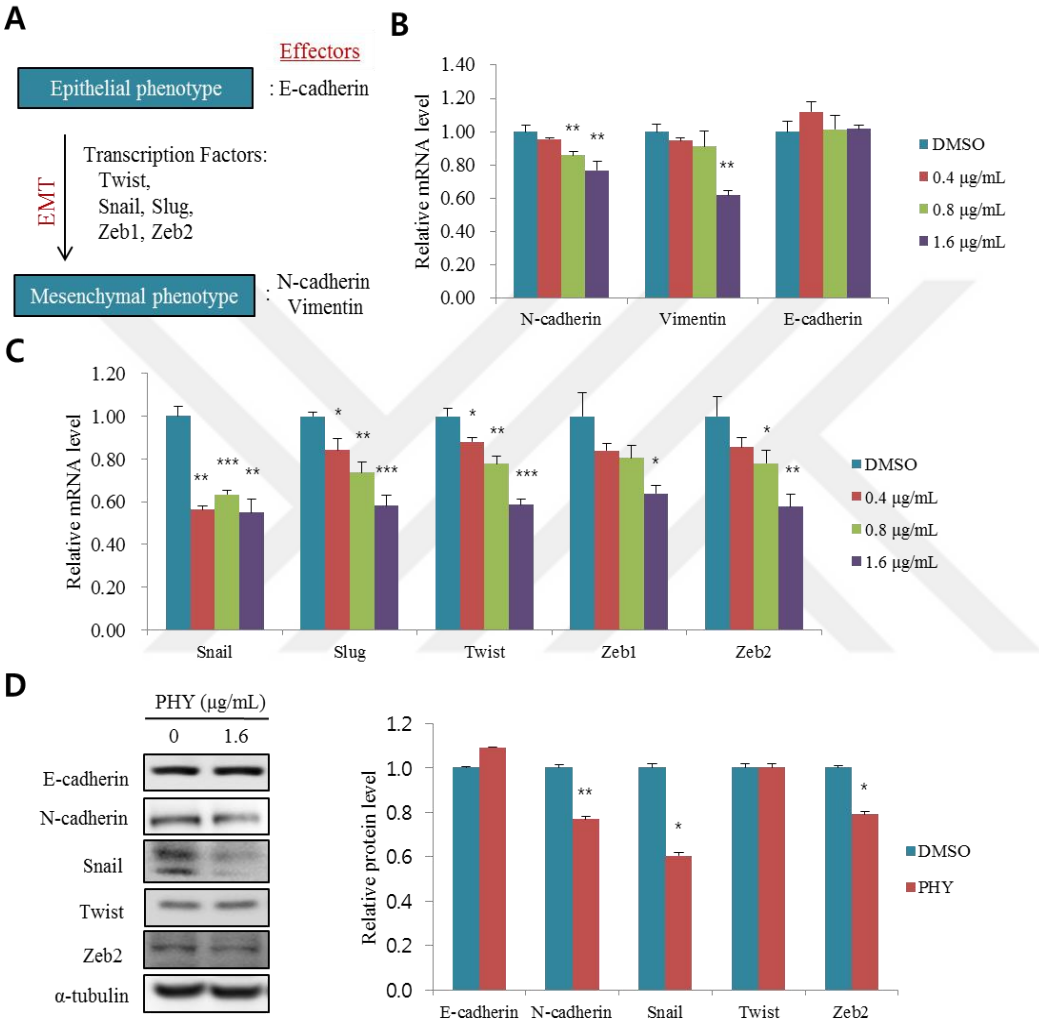
A
Effectors
Epithelial phenotype
: E-cadherin
EMT
Transcription Factors:
Twist,
Snail, Slug,
Zeb1, Zeb2
Mesenchymal phenotype
: N-cadherin
Vimentin
B
Relative mRNA level
1.40
1.20
1.00
0.80
0.60
0.40
0.20
0.00
N-cadherin
Vimentin
E-cadherin
DMSO
0.4 μg/mL
0.8 μg/mL
1.6 μg/mL
C
Relative mRNA level
1.20
1.00
0.80
0.60
0.40
0.20
0.00
Snail
Slug
Twist
Zeb1
Zeb2
DMSO
0.4 μg/mL
0.8 μg/mL
1.6 μg/mL
D
PHY (μg/mL)
0
1.6
E-cadherin
N-cadherin
Snail
Twist
Zeb2
α-tubulin
Relative protein level
1.2
1.0
0.8
0.6
0.4
0.2
0.0
E-cadherin
N-cadherin
Snail
Twist
Zeb2
DMSO
PHY

Figure 1.7. PHY modulates expression of EMT effectors by downregulating transcription factors. To elucidate the mechanisms by which PHY suppresses the motility of CRC cells, expression of EMT-related genes in Caco2 cells was analysed by qRT-PCR and western blotting. (A) Schematic model of EMT. (B) Relative mRNA expression of EMT effectors (N-cadherin, vimentin, and E-cadherin) in Caco2 cells treated with non-toxic concentrations (0.4, 0.8 and 1.6 µg/mL) of PHY. (C) Relative mRNA expression of EMT transcription factors (Snail, Slug, Twist, Zeb1 and Zeb2) in Caco2 cells treated with non-toxic concentrations (0.4, 0.8 and 1.6 µg/mL) of PHY. mRNA levels were normalised against that of GAPDH. (D) Protein expression of N-cadherin, E-cadherin, Slug, Twist and Zeb2. α-Tubulin served as a loading control. Data represent the mean ± standard error of the mean, n = 3. * $P < 0.05$; ** $P < 0.01$; *** $P < 0.001$.

1.3.5. PHY reduces actin-based cell motility

To clarify the mechanisms by which PHY modulates cell migration and invasion, we performed pathway-focused gene expression analysis using the Human Cell Motility RT² Profiler™ PCR Array. Figure 1.8A schematically shows the linkages between genes involved in the cell motility pathway that were downregulated or upregulated in Caco2 cells treated with 1.6 μg/mL PHY. PHY downregulated vascular endothelial growth factor A (VEGFA), phosphatidylinositol-4,5-bisphosphate 3-kinase catalytic subunit alpha (PIK3CA), Rac family small GTPase 1 (RAC1), cell division cycle 42 (CDC42), WAS protein family, member 1 (WASF1), WAS protein family, member 2 (WASF2), profilin 1 (PFN1), actin-related protein 2 (ARP2), actin-related protein 3 (ARP3) and calpain 2 (CAPN2), but upregulated vinculin (VCL) (Fig. 1.8B). The Arp2/3 complex nucleates actin polymerisation and directly regulates the polymerisation reaction by interacting with Wiskott–Aldrich-syndrome-related protein (WASP)/WAVE family proteins (Rohatgi et al., 1999). The WASP and ARP2/3 genes are downstream of Rho GTPases genes (Otsubo et al., 2004). Activation of PIK3CA (also known as PI3K) is sufficient to induce the motile phenotype and is necessary for cell motility using Rho GTPases, including Cdc42 and Rac (Keely et al., 1997). PI3K activity was recently reported to be required for many effects of VEGFA, such as those on cell proliferation, migration and survival (Graupera et al., 2008).

Taken together, our data suggest that PHY reduces actin-based cell motility driven by VEGFA.

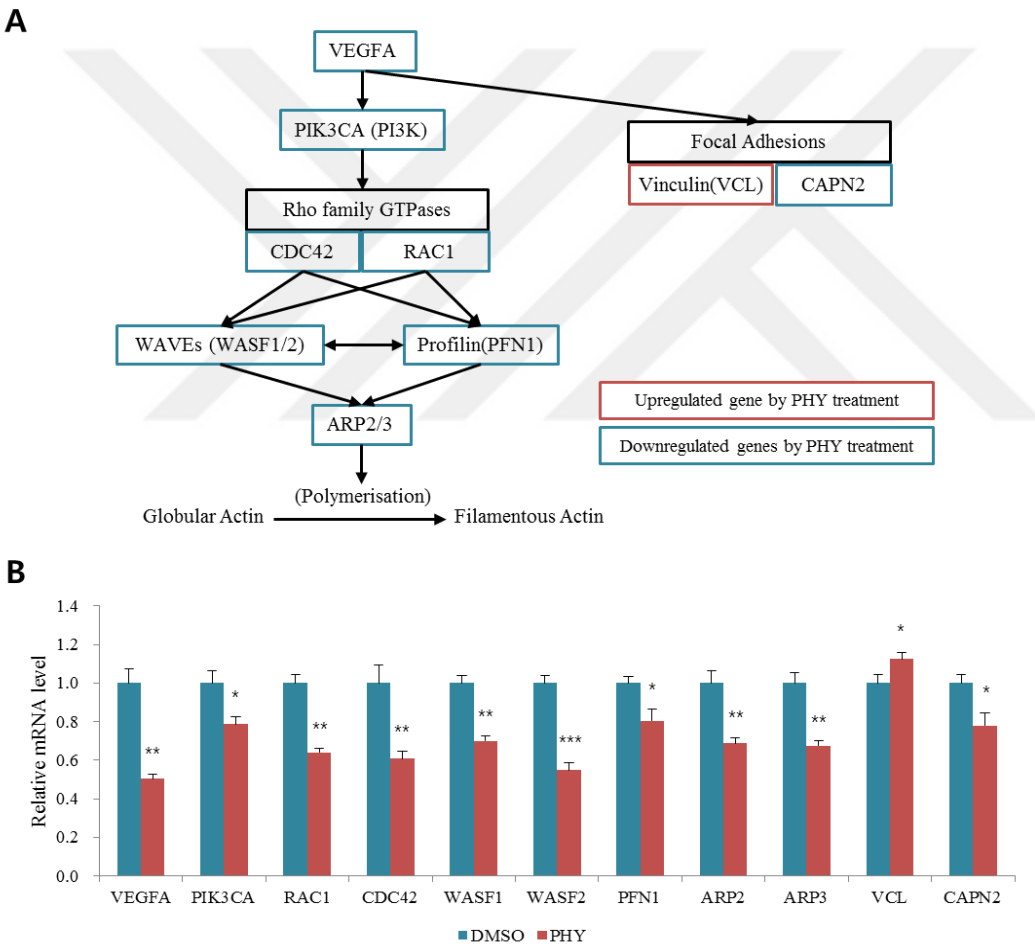

Figure 1.8. PHY reduces actin-based motility of CRC cells. Pathway-focused gene expression analysis using the Human Cell Motility RT² Profiler™ PCR Array was performed to elucidate the mechanisms by which PHY modulates cell migration and invasion. (A) Schematic of the linkages between genes that were upregulated or downregulated in Caco2 cells treated with 1.6 μg/mL PHY. (B) Quantitative analysis of mRNA expression of VEGFA, PIK2CA, RAC1, CDC42, WASF1, WASF2, PFN1, ARP2, ARP3, CAPN2 and VCL in Caco2 cells treated with 1.6 μg/mL PHY. Data represent the mean ± standard error of the mean, n = 3. * $P < 0.05$; ** $P < 0.01$; *** $P < 0.001$.

1.3.6. PHY modulates expression of KAI1 C-terminal-interacting tetraspanin (KITENIN) and KAI1, and downregulates downstream transcription factors

The metastasis-enhancing gene KITENIN is highly expressed in sporadic CRCs. Moreover, epidermal growth factor increases KITENIN-mediated AP-1 activity (Bae et al., 2014). KAI1 suppresses metastasis of a variety of solid tumours and has an inverse relationship with KITENIN (Fig. 1.9A) (Bae et al., 2018). We previously reported that PHY dose-dependently decreases KITENIN-mediated AP-1 activity (Yang et al., 2015). PHY suppressed mRNA expression of KITENIN and significantly upregulated that of KAI1 in Caco2 cells (Fig. 1.9B). Consistently, PHY decreased protein expression of KITENIN (Fig. 1.9C). Consequently, total and nuclear distribution of AP-1 transcription factors, c-Jun, c-Fos as well as phosphor-c-Jun, are decreased by PHY (Fig. 1.9D). Taken together, these results show that PHY inhibits cell motility by modulating expression of KITENIN and KAI1, and by downregulating downstream transcription factors.

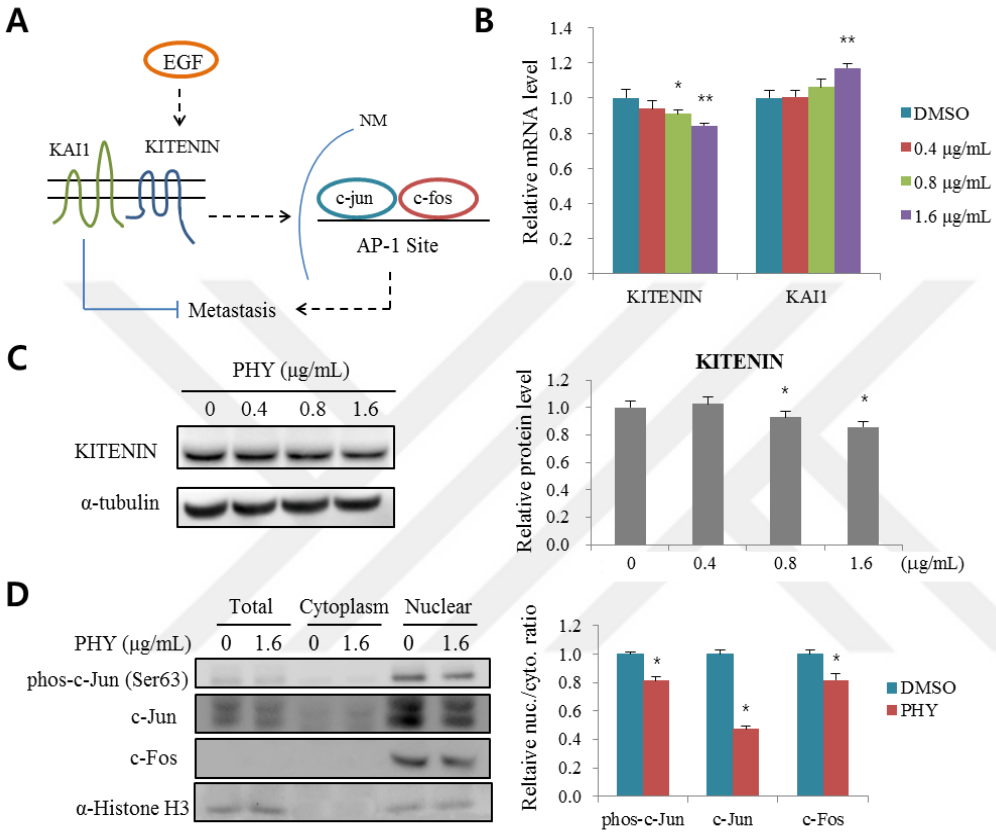
A
EGF
KAI1
KITENIN
NM
c-jun
c-fos
AP-1 Site
Metastasis
B
Relative mRNA level
1.4
1.2
1.0
0.8
0.6
0.4
0.2
0.0
*
**
**
KITENIN
KAI1
DMSO
0.4 μg/mL
0.8 μg/mL
1.6 μg/mL
C
PHY (μg/mL)
0
0.4
0.8
1.6
KITENIN
α-tubulin
KITENIN
Relative protein level
1.2
1.0
0.8
0.6
0.4
0.2
0.0
*
*
0
0.4
0.8
1.6
(μg/mL)
D
Total
Cytoplasm
Nuclear
PHY (μg/mL)
0
1.6
0
1.6
0
1.6
phos-c-Jun (Ser63)
c-Jun
c-Fos
α-Histone H3
Reltaive nuc./cyto. ratio
1.2
1.0
0.8
0.6
0.4
0.2
0.0
*
*
*
phos-c-Jun
c-Jun
c-Fos
DMSO
PHY

Figure 1.9. PHY modulates KITENIN- mediated oncogenic signals. To elucidate whether PHY affects the KITENIN- and β-catenin-mediated oncogenic signals in CRC cells, expression of KITENIN, KAI1, β-catenin and their downstream effectors in Caco2 cells was analysed by qRT-PCR and Western blotting. (A) Shematic illustration of KITENIN-mediated oncogenic signals. NM, nuclear membrane. (B) Quantitative analysis of mRNA expression of KITENIN and KAI1 in Caco2 treated with non-toxic concentrations (0.4, 0.8 and 1.6 µg/mL) of PHY. (C) PHY decreases protein expression of KITENIN in Caco2 cells. (D) Western blot analysis of total cytoplasmic and nuclear phospho-c-jun (Ser63), c-jun and c-fos in Caco2 cells. α-Histone 3 served as a loading control. Data represent the mean ± standard error of the mean, n = 3. * $P < 0.05$; ** $P < 0.01$; *** $P < 0.001$.

1.3.7. PHY downregulates β-catenin and downstream target genes

Deregulation of Wnt and its downstream effectors promotes cancer initiation, growth and metastasis (Tai et al., 2015). Wnt/β-catenin (canonical pathway) is mutated in ~90% of CRCs (Sebio et al., 2014). We analysed whether PHY affects the Wnt/β-catenin pathway. PHY decreased β-catenin expression (Fig. 1.10A and 1.10B). Activation of β-catenin also modulates downstream target genes, including cyclin-D1 and c-Myc (Stewart, 2014). PHY decreased mRNA expression of cyclin-D1 and c-Myc in CRC cells (Fig. 1. 10C). These findings indicate that PHY downregulates EMT markers and elicits anti-tumour activity via the Wnt/β-catenin cascade.

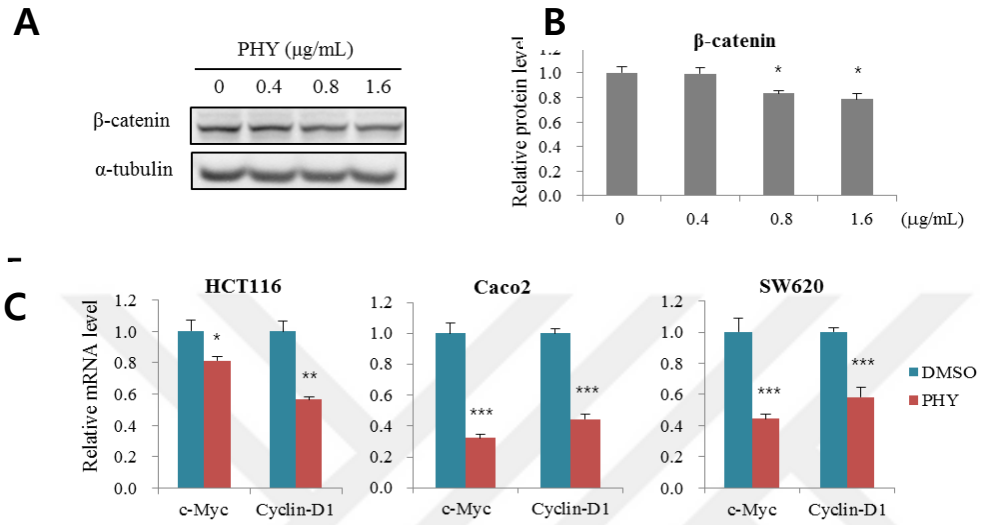

Figure 1. 10. PHY modulates β-catenin-mediated oncogenic signals. (A-B) Treatment with non-toxic concentrations (0.4, 0.8 and 1.6 μg/mL) of PHY decreases protein expression of β-catenin in Caco2 cells. α-Tubulin served as a loading control (C) Quantitative analysis of c-Myc and cyclin-D1 mRNA expression in HCT116, Caco2 and SW620 cells treated with 1.6 μg/mL PHY. Data represent the mean ± standard error of the mean, n = 3. * $P < 0.05$; ** $P < 0.01$; *** $P < 0.001$.

1.3.8. PHY inhibits the growth of CRC xenografts in vivo

To evaluate the effect of PHY in vivo, firstly we determined the bioavailability of PHY to decide required dosage for in vivo study. LC-MS/MS analysis revealed that intraperitoneal administration of 30 mg/kg PHY in mice showed 2.91 ± 0.0089 μM (~1.18 μg/mL) in plasma after 24 h (Fig. 1.11A). Although this is within the concentration range used in vitro, the 30 mg/kg dosage was not available due to toxicity probably because it will give ~44 mg/mL of PHY, which is above IC_{50} values, at the time of injection. Thereafter, CT26 xenograft murine models were generated. After 10 days, tumour-bearing mice were intraperitoneally injected with DMSO (control) or PHY (7.5 mg/kg) and this injection was repeated once every 2 days for ~3 weeks. Tumour volume and weight were 55% and 57% lower in PHY-treated mice than in control mice, respectively. PHY did not reduce the body weight of mice, suggesting that it has no toxic effect (Fig. 1. 11B – 1. 11F). Together, these results demonstrate that PHY inhibits the growth of CT26 xenografts in vivo.

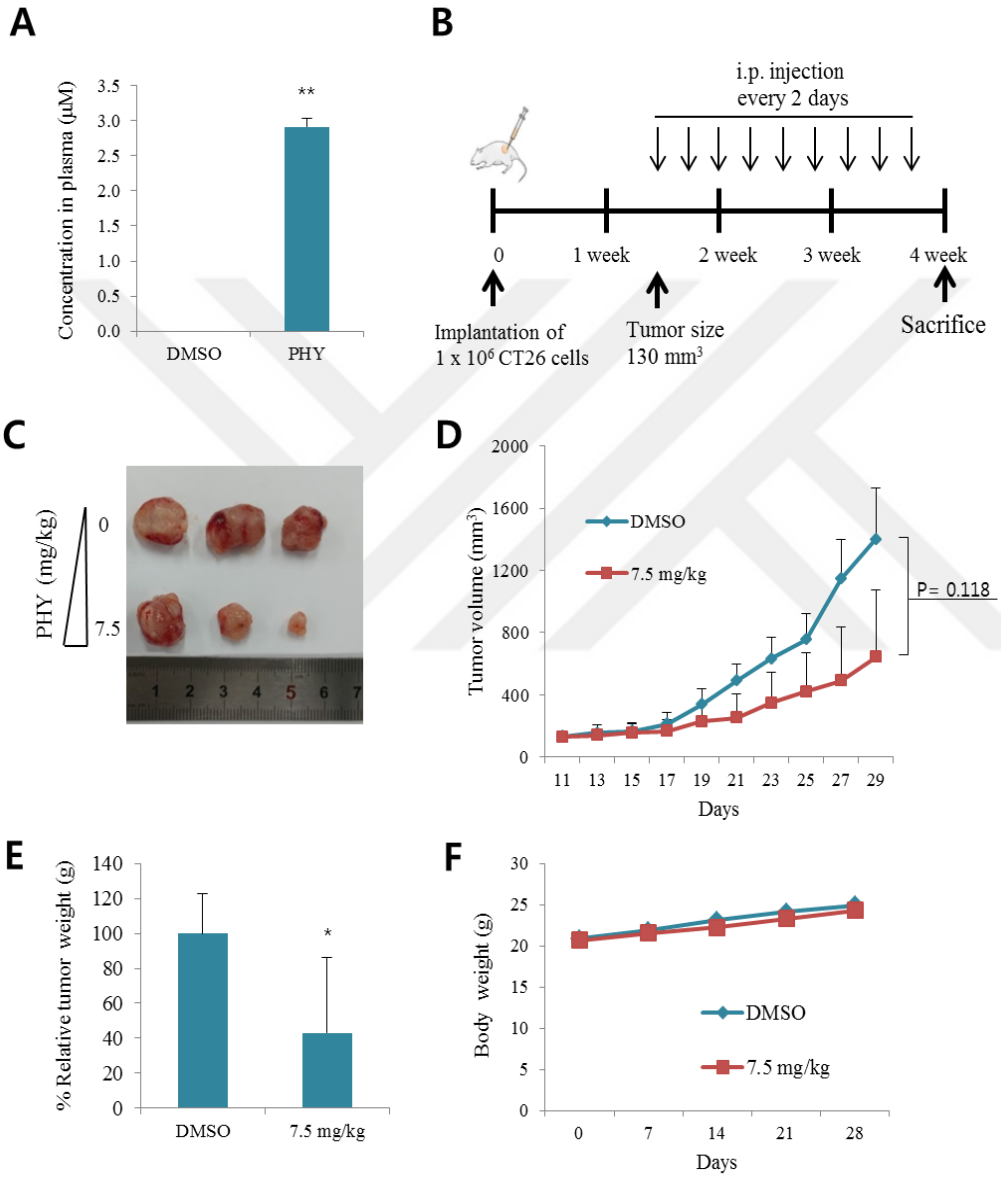
A
Concentration in plasma (μM)
3.5
3.0
2.5
2.0
1.5
1.0
0.5
0.0
**
DMSO
PHY
B
i.p. injection
every 2 days
0
1 week
2 week
3 week
4 week
Implantation of
1 x 10⁶ CT26 cells
Tumor size
130 mm³
Sacrifice
C
PHY (mg/kg)
0
7.5
D
Tumor volume (mm³)
2000
1600
1200
800
400
0
DMSO
7.5 mg/kg
P= 0.118
11 13 15 17 19 21 23 25 27 29
Days
E
% Relative tumor weight (g)
140
120
100
80
60
40
20
0
*
DMSO
7.5 mg/kg
F
Body weight (g)
30
25
20
15
10
5
0
DMSO
7.5 mg/kg
0 7 14 21 28
Days

Figure 1. 11. PHY inhibits the growth of CT26 xenografts *in vivo*. (A) PHY concentration in plasma detected by LC-MS/MS. (B) Schedule of the *in vivo* experiment. A total of 1×10^6 CT26 cells were implanted beneath the skin of each mouse (n=6). Ten days later, mice were interperitoneally (i.p.) injected with PHY (7.5 mg/kg body weight) and this injection was repeated every 2 days for ~3 weeks. (B) A representative photograph of xenografts collected from sacrificed mice at the end of the treatment period. (C) Tumour volumes when each injection was delivered. (D) Relative percentage of tumour weight. (E) Body weight of control and PHY-treated mice. Data represent the mean ± standard error of the mean. * $P < 0.05$; ** $P < 0.01$.

1.4. Discussion

CRC is the third most common cancer in men (10.0% of all cancers) and the second most common cancer in women (9.2% of all cancers) worldwide. Moreover, CRC is the fourth most common cause of cancer-related death globally, accounting for more than 1.2 million new cases in 2012 (Ferlay et al., 2015). Although improved treatment strategies involving surgery, chemotherapy and radiotherapy have increased overall survival rates in the early stages, 40–50% of all CRC patients exhibit metastasis at the time of diagnosis or as recurrent disease upon intended curative therapy (Cao et al., 2015). Moreover, the treatment strategies are toxic, which has led to investigations of complementary and alternative medicines. Natural compounds derived from plants have acquired much interest because they are less toxic than chemotherapeutic drugs (Sikander et al., 2016).

Lichens are symbiotic organisms that synthesise bioactive metabolites with a variety of effects (Zhou et al., 2017). PHY is an effective metabolite isolated from the Chile lichen *Pseudocyphellaria* sp. We previously reported that PHY inhibits the motility of lung cancer cells and elucidated the underlying mechanism (Yang et al., 2015). Here, PHY suppressed the growth and motility of CRC cells via novel mechanisms. The study makes the following findings: 1) treatment with toxic concentrations of PHY decreases the viability of CRC cells by inducing apoptosis; 2) PHY suppresses the motility and tumorigenic potential of CRC cells *in vitro*; 3)

PHY decreases the motility of CRC cells by modulating EMT and actin polymerisation; 4) PHY modulates KITENIN- and b-catenin-mediated oncogenic signals; and 5) PHY suppresses the tumorigenic potential of CRC cells *in vivo* without eliciting any toxic effects at the tested dosage. Collectively, this study demonstrates the therapeutic potential of PHY to control the growth and metastatic behaviour of CRC cells.

Nuclear condensation is used to differentiate between apoptotic and normal/necrotic cells (Crowley et al., 2016b). Phosphatidylserine translocates from the inner to the outer leaflet of the plasma membrane upon activation of apoptosis (Koopman et al., 1994). Fluorescently labelled Annexin V can be used to detect phosphatidylserine on the surface of apoptotic cells. Co-staining with Annexin V and PI, another fluorescent dye, can distinguish between necrotic and apoptotic cells (Crowley et al., 2016a). The nuclear polymerase PARP is essential for DNA repair in response to cellular stresses. Cleavage of PARP by caspases facilitates cellular disassembly and is a marker of apoptotic cells (Chaitanya et al., 2010). PHY was cytotoxic to all the CRC cell lines used in the current study (Fig. 1.1). Hoechst staining showed that PHY induced nuclear condensation in CRC cells. Annexin V/PI staining and analysis of PARP and caspase-3 activities confirmed that PHY induced apoptosis in CRC cells (Fig. 1.2).

EMT is a crucial and complex phenomenon in cancer invasion and metastasis (Cao et al., 2015). EMT-related transcription factors (Snail1, Slug, Twist, Zeb1 and Zeb2) and mesenchymal markers (N-cadherin and vimentin) are overexpressed in CRC and this is associated with an increased rate of cancer recurrence and decreased survival of CRC patients (Vu and Datta, 2017). Inhibition of EMT is an attractive therapeutic approach that can significantly alter disease outcomes (Gulhati et al., 2011). PHY decreased expression of N-cadherin, vimentin, Snail, Slug, Twist, Zeb1 and Zeb2 in the present study (Fig. 1.4). This suggests that PHY suppresses the motility of CRC cells by modulating EMT.

VEGF initiates essential steps of vasculogenesis and angiogenesis, including matrix degradation and proliferation and migration of endothelial cells, and is essential to drive actin-based motility (Rousseau et al., 2000). PI3K activity is required for many effects of VEGFA, such as those on cell proliferation, migration and survival (Graupera et al., 2008). PI3K and Rho GTPases, including Cdc42 and Rac1, are part of a positive feedback loop that stimulates WASP/WAVE proteins (Hanna and El-Sibai, 2013). This cascade activates the Arp2/3 complex, leading to reorganisation of the actin cytoskeleton and formation of filopodia and lamellipodia during cell motility (Kurisu and Takenawa, 2010). Consistently, PHY downregulated mRNA expression of VEGFA, PIK3CA, CDC42, RAC1, WAVE1/2 and ARP2/3, which are part of the actin-based cell motility pathway

driven by VEGF (Fig. 1.5). VEGF signalling also regulates angiogenesis; therefore, further study is required to evaluate the anti-angiogenic activity of PHY in endothelial cells.

KAI1 expression is inversely correlated with cancer metastasis (Miller et al., 2018). mRNA and protein expression of KAI1 is decreased in advanced stages of CRC and is lost during metastasis (Maurer et al., 1999). KITENIN is associated with progression of human CRC, including invasion and metastasis (Lee et al., 2011). Increased expression of KITENIN and decreased expression of wild-type KAI1 may be molecular markers of cancer metastasis (Lee et al., 2004). We previously reported that PHY suppresses KITENIN-mediated AP-1 activity in a dose-dependent manner (Yang et al., 2015). The current study demonstrates that PHY suppressed protein and mRNA expression of KITENIN and significantly upregulated mRNA expression of KAI1 in CRC cells. Moreover, PHY downregulated expression of the AP-1 transcription factors c-Jun and c-Fos in CRC cells. Taken together, our findings suggest that PHY suppresses metastasis by inhibiting expression of KITENIN and downstream targets, and by inducing expression of KAI1 (Fig. 1.6A–1.6D).

Wnt signalling pathways are essential for numerous biological processes, including embryogenesis, cell cycle modulation, inflammatory changes and cancer (Tai et al. 2015). These pathways are subdivided into the canonical β-catenin-

dependent pathway and the noncanonical β-catenin-independent pathway (Novellasdemunt et al., 2015). Wnt/β-catenin (canonical pathway) is mutated in ~90% of CRCs (Sebio et al., 2014). Moreover, a recent study reported that the Wnt/β-catenin pathway induces EMT in CRC cells (Qi et al., 2016). As downstream effectors of the Wnt/β-catenin pathway, C-Myc and cyclin-D1 are important for the initiation and progression of CRC *in vitro* and *in vivo* (Kim et al., 2015; Tögel et al., 2016). Our results demonstrate that PHY suppressed expression of β-catenin and its downstream genes c-Myc and cyclin-D1 (Fig. 1.7), which may underlie the anti-tumour and EMT-suppressive effects of PHY.

PHY suppressed the growth of CRC cells *in vitro* and we sought to confirm this finding in a xenograft model of CRC. To begin with, PHY concentration in plasma was detected by LC-MS/MS analysis and injection dosage for *in vivo* study was determined. Thereafter, 1×10^6 CT26 cells were implanted subcutaneously into the right flank of each mouse and generated tumour. PHY (7.5 mg/kg body weight) was intraperitoneally injected once every 2 days for ~3 weeks. *In vivo* study indicated that PHY inhibited growth of CT26 cells in mice. In addition, body weight did not differ between control and PHY-treated mice. These findings indicate that PHY inhibits the growth of CRC xenografts without eliciting toxic effects at given dosage.

In summary, our experiments *in vitro* and *in vivo* demonstrate that PHY inhibits the proliferation, motility and tumorigenesis of CRC cells and induces their apoptosis. A further study is required to evaluate the potential anticancer activity of PHY in various orthotopic cancer models.

Chapter II. Physciosporin suppresses breast cancer growth and induces metabolic dysfunction

2. Physciosporin Suppresses Breast Cancer Growth and Induces Metabolic Dysfunction

2.1. Introduction

Cancer is one of the major causes of death worldwide and clearly rank as a growing global health problem in 21st century. In 2018, it was estimated 18.1 million new cancer cases and 9.6 million mortality from cancer worldwide (Li et al., 2020; Zhang et al., 2020). Although widespread screening programs and greatly improved treatment of early disease, BC is second leading cause of cancer death among women after lung cancer (Komorowski et al., 2020; Mazo et al., 2020).

Reprograming of energy metabolism in cancer is one of the hallmarks of cancer. To supply the energy needed for anabolic reactions, cancer cells use aerobic glycolysis, known as the Warburg effect. Aerobic glycolysis in cancers is the combined result of oncogenes, tumor suppressors, a hypoxic microenvironment, mtDNA mutations and others (Jang et al., 2013; Vernieri et al., 2016). In addition to oncogenic activities of c-Myc, PI3K/AKT, HIF-1, NF-κB and STATs, they act as regulator and/or co-activator of glycolytic enzymes such as Glut1, HK2, PKM2 and LDHA (Jang et al., 2013; Woolf et al., 2016). Meanwhile, recent studies revealed that those glycolytic enzymes, specially PKM2, participate in tumor progression independent of their canonical metabolic roles (Yu and Li, 2017).

Therefore, targeting on multiple enzymes in the glycolysis pathway have been identified as promising targets for cancer therapy and drug discovery.

Lichens are symbiotic associations of fungi and photosynthetic partners (algae and cyanobacteria). They synthesize a wide range of secondary metabolites to provide defense against biotic and abiotic stress conditions (Nash, 2008). For centuries in traditional medicine, lichens have been commonly used for treating wounds, skin disorders, respiratory and digestive problems (Crawford, 2015; Tas et al., 2019; Yang et al., 2018b). Moreover, lichens have great interest as a source of therapeutic agents to treat numerous diseases including cancer in current research (Taş et al., 2019a; Yang et al., 2018a; Zhou et al., 2017).

Physciosporin (PHY) is a depsidone-derived lichen metabolite found in several species of the genus Pseudocyphellaria (Huneck and Yoshimura, 1996). Previously, we have demonstrated that PHY has anti-metastatic, anti-proliferative and anti-tumor activity on colorectal and lung cancer cell with molecular mechanism of action (Taş et al., 2019a; Yang et al., 2015). Here, the aim of the current research was to assess the effects of PHY on growth and metabolic activity of BC cells and further to investigate the possible molecular mechanisms.

2.2. Materials and Methods

2.2.1. Cell culture

Human BC cells MDA-MB-231 and MCF-7, mouse mammary carcinoma cells 4T1-iRFP and non-tumorigenic human breast epithelial cells MCF10A cells were used in this research. All human cells were cultured in Dulbecco's Modified Eagle Medium (DMEM) (Gen Depot, USA) supplemented with 10% FBS and 1% Penicillin-Streptomycin solution and mouse cancer cell was cultured in Roswell Park Memorial Institute (RPMI) medium (Gen Depot, USA) supplemented with 10% FBS and 1% Penicillin-Streptomycin solution. Cells were incubated in 5% CO2 in a humidified atmosphere at 37 °C.

2.2.2. MTT assay

PHY was dissolved in DMSO (Sigma Aldrich, St. Louis, USA) and diluted into 5 different concentrations (3.125, 6.25, 12.5, 25 and 50 µg/mL). 2.5-7.5×10^3 cells/well were seeded in 96 well plate. After overnight incubation, cells were treated with DMSO or PHY at indicated concentrations for 48 h. Once treatment was completed, 15 µL methyl thiazolyl tetrazolium (MTT) (Sigma Aldrich, USA) reagent were added and then incubated for additional 4 h. After incubation, supernatants were carefully removed, and formazan crystals were dissolved in 150 µL DMSO. The absorbance was measured at 570 nm using microplate reader with

Gen 5 (2.03.1) software (BioTek, VT, USA). The percentage of cell viability formula;

$$\frac{\text{Optical Density (OD) of the sample treated x 100}}{\text{OD of the control treated}}$$

IC_{50} values were calculated using the (Statistical Package for Social Science) SPSS software.

2.2.3. Scratch wounding migration assay

Scratch wounding migration assay was detected by the IncuCyte HD system (IncuCyte ZOOM, Essen BioScience, USA). MDA-MB-231 cells were plated into Essen ImageLock 96-well plates at the number of 2×10^4 cells per well. Cells were then serum-starved for six hours and the monolayer of confluent cells was scratched using Essen Wound Maker to generate wound. After wounding, debris was removed by PBS washing for two times and incubated in 2% medium with different concentration s of PHY. Typical kinetic updates were recorded at 3 h intervals for the duration of 48 h. The data were analyzed using an integrated metric of Incucyte Software, relative wound density (RWD). This algorithm measures cell density in the wound area relative to the cell density outside of the wound area at each set time point.

2.2.4. Clonogenic assay

The human BC cells were cells were seeded into six-well plates at 500-1000 cells/well in 2 mL of DMEM and incubated to allow attachment. After 48 h treatment with PHY (1.5, 3 and 6 µg/mL), media containing PHY was replaced with fresh medium and then incubated for 2-3 weeks. Colonies were fixed by 100% methanol, stained with 0.5% crystal violet, and quantified under a microscope.

2.2.5. Soft agar colony formation assay

The BC cells (2.5×10^3) were suspended in 1 mL of 0.35% upper layer (50:50 – agarose diluted in 2×DMEM) added onto 1 mL of 0.5% base layer (50:50 – agarose diluted in 2× DMEM) in 12 well plate and cultured for 3 weeks. Once in three days, feeder medium (culture medium containing treatment sample with represented concentrations) were refreshed. Colony area was measured by Nikon Eclipse 400 fluorescence microscope software in randomly selected five fields per well. Data was represented after three repetitions.

2.2.6. Flow cytometric analysis

For Anexin-V-FITC & PI double staining, the human BC cells were seeded into six- well plates in the number of 2×10^5 cells/well, cultured overnight and then treated with the toxic dose of PHY (30 µg/mL) for 48 h. After incubation, cells were trypsinized, washed with cold PBS and centrifuged (1200 rpm, 5 min). To

determine the apoptotic populations, firstly the cells were resuspend with 1× Binding Buffer and incubated on ice in the presence of Annexin-V-FITC (2.5 μL) and PI (5 μL)solution for 15 min in the dark and analyzed.

For cell cycle, human BC cells were seeded in six-well plates in the number of 2×10^5 cells/well, cultured overnight and then treated with PHY for 48 h. Then, cells were washed with washing solution. First, trypsin solution was added and incubated for 10 min and then RNase inhibitor was added and incubated for 10 min at room temperature. Next, the samples were centrifuged, the supernatants were removed, and the pellets were resuspended in 100 mL of 4 mg/mL PI (Sigma-Aldrich,St. Louis, MO, USA) and incubated for 2 h in the dark at 4◦C. Subsequently, the stained cells were analyzed by Cytoflex flow cytometer (Beckman Coulter Life Sciences, Indianapolis, USA) and CytExpert 2.0.0.152 software.

2.2.7. Extracellular acidification rate (ECAR) and oxygen consumption rate (OCR) measurement

The XF96 extracellular flux analyzer (Agilent, Santa Clara, CA) was used to detect real-time changes in extracellular acidification rate (ECAR) and oxygen consumption rate (OCR). Briefly, cells were seeded at a density of 5×10^3 cells per well and cultured overnight in growth medium containing 2% fetal bovine serum. Then, cells were treated with different concentrations of PHY for 48 h. For ECAR

analysis (Glycolytic Rate Assay), 0.5 μM Rotenone (Rot) + antimycin A (AA) and 50 mM 2-deoxy-d-glucose (2-DG) and for OCR analysis (Cell Mito Stress Test), 1 μM oligomycin, 1 μM carbonyl cyanide 4-(trifluoromethoxy) phenylhydrazone (FCCP), 0.5 μM Rotenone (Rot) + antimycin A (AA) were loaded into hydrated sensor cartridge. On the analyze day, cells medium was changed to bicarbonate-free low-buffered assay medium supplemented with glucose, sodium pyruvate, and glutamine. After cells incubated for 1 h at 37 °C in a non-CO2 incubator, oxygen consumption rate and extracellular acidification rate were measured by using the Seahorse XF instrument (Agilent, Santa Clara, CA). The results were automatically calculated by the Wave software (Agilent, Santa Clara, CA).

2.2.8. Quantitative Real-Time PCR

Total RNA was isolated from BC cells by using RNAiso Plus (TaKaRa, Otsu, Japan) according to manufacturer's instructions. 1 μg of RNA was converted to cDNA by M-MLV reverse transcriptase (Invitrogen, Carlsbad, USA). Relative expressions of candidate genes was analyzed using SYBR green (Enzynomics, Seoul, Korea). The primers used for real time PCR were listed in the Table S2. Real-time PCR and analysis were performed by CFX (Bio-Rad, Hercules, CA, USA).

Table 2. The primers used for qRT-PCR.

Gene Symbol	Primers sequences		Accession	Product Length (bp)
	For (5'-3')	Rev (5'-3')		
GLUT1	CTTTGTGGCCTTCTTTGAAGT	CCACACAGTTGCTCCACAT	NM_006516.3	168
HIF1A	ATCCATGTGACCATGAGGAAATG	TCGGCTAGTTAGGGTACACTTC	NM_181054.3	201
LDHA	TGGCCTGTGCCATCAGTATC	TTCCAAGCCACGTAGGTCAA	NM_001165415.2	239
PKM2	GCTGCCATCTACCACTTGC	CCAGACTTGGTGAGGACGATT	NM_001791.3	200
GAPDH	ATCACCATCTTC CAGGAGCGA	AGTTGTCATGGATGACCTTGGC	NM_002046.6	283

2.2.9. Western blotting

Cells were seeded into 6 well plates for 12 h, and then treated with toxic (30 µg/mL) or non-toxic concentrations (1.5, 3, and 6 µg/mL) of PHY for 24 and 48 h, washed twice with cold PBS, lysed in lysis buffer and extracted the whole cell proteins. The protein concentrations were determined by bicinchoninic acid (BCA) protein assay (Thermo Fisher Sciences, USA). The antibodies used were purchased from Cell signaling Technology (α-tubulin, β-catenin, Bax, Bcl-xL, caspase-3, GAPDH, Glut1, HIF-1α, LDHA, NF-kB, P-NF-kB, PARP, PKM2, STAT3 and P-STAT3), Santa Cruz (c-Myc), MERCK (cyclin-D1), and Sigma-Aldrich (β-actin). Antibodies were detected with horseradish peroxidase-conjugated secondary antibody (Thermo Fisher Sciences, USA) using Immobilon Western Chemiluminescent HRP Substrate Kit (MILLIPORE) and luminescence imaging (iBright™ FL1000 Imaging System, Thermo Fisher Sciences, USA). Bands were measured by Multi- Gauge 3.0 and their relative density calculated based on the density of the α-tubulin bands in each sample. Values were expressed as arbitrary densitometric units corresponding to signal intensity.

2.2.10. In vivo antitumor study

Six-week-old pathogen-free conditioned female BALB/c mice were obtained from Orient Company (Seongnam, Korea). The handling of animals and all in vivo experiments were performed according to the Guiding Principles in the Care and Use of Animals (DHEW publication, NIH 80-23). The Sunchon National University Research Institutional Animal Care and Use Committee approved the experimental protocol. Orthotopic BC xenografts were established using 4T1-iRFP cells. 4T1-iRFP cells were trypsinized and suspended in phosphate buffered saline (PBS), and the cell suspension (2×10^5 cells in 0.1 mL of PBS/mouse) was injected into mammary fat pads of the BALB/c mice (n=10). For orthotopic BC xenografts model, each animal was anesthetized by subcutenously. A small incision was made between the fourth nipple and the midline with a scissor and moistened with PBS pH 7.4. The mammary fat pad was exposed by using a tweezer to perform injection easily. After homogenized the cell mixture, it was injected into mammary fat pad by insulin syringe. The incision was sutured by using a needle driver and sterilized. 9 days after tumor cell injection, at which time the primary tumor had reached approximately 60 mm^3 and the mice were divided into two experimental groups. While vehicle (DMSO/ DMEM) was injected to the control group, another group was treated with Physciosporin at the dose of 5 mg/kg body weight by intraperitoneal (i.p.) injection every three days. The tumor volumes were

calculated the following formula: $mm^3=0.5\times L\times W^2$, wherein L is length, W is width, and mm is millimeter. Bioimaging was performed immediately using fluorescence-labeled organism bioimaging instrument (FOBI) system (Neoscience, Suwon, Korea). Mouse tumor tissues were isolated after sacrifice, and tumor weight was determined in each sample.

2.2.11. Statistical analysis

All in vitro experiments were performed in triplicates. Data were expressed as means ± standard deviation. P-values of <0.05 are considered statistically significant. All statistical analyses were performed using the SPSS and Sigma Plot software.

2.3. Results

2.3.1. PHY decreases BC cell growth

Initially, we investigated whether exposing breast cell lines to different concentration of PHY affected anti-proliferative activity by performing MTT assay. We used four breast cell lines including MDA-MB-231, MCF-7, 4T1-iRFP (mouse) and MCF10A (non-tumorigenic human) cells. While MDA-MB-231 (triple negative BC cell) accounts for ~12% of all BC cases, MCF-7 (ER+ BC cell) is the most common subtype, accounting for ~70% (Ogrodzinski et al., 2017). Here, we observed that PHY had a dose dependent inhibitory effect on breast cells in the range of 3-50 µg/mL for up to 48 h treatment. The IC_{50} of PHY was 27.3 µg/mL in MDA-MB-231 cells, 24.1 µg/mL in MCF-7 and 9.7 µg/mL in 4T1-iRFP after PHY treatment for 48h. Moreover, PHY showed a lower cytotoxicity on the viability on MCF10A cell lines (IC_{50}: 31.0 µg/mL) (Fig.2.1A-B).

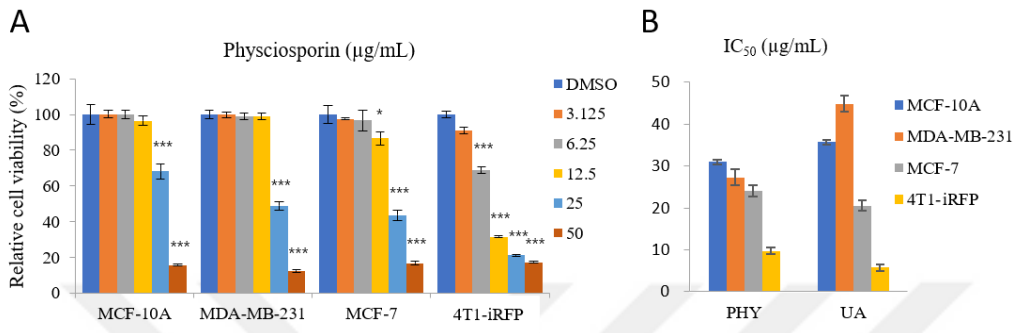

Figure 2.1. PHY inhibits the Breast Cancer cell (BC) viability in a dose-dependent manner. (A) Non-cancer MCF-10A cell and three different BC cells (MDA-MB-231, MCF-7 and 4T1-iRFP) were seeded in 96-well plates, and after 12 h, they were treated with PHY concentrations (3, 6, 12.5, 25 and 50 µg/mL) for 48 h. The cell viabilities were measured by MTT assays (B) Calculated IC_{50} values in response to treatment with PHY and positive control usnic acid (UA). Data represents the mean ± standard error of the mean, n = 3. * $P < 0.05$; *** $P < 0.001$.

2.3.2. PHY elicits cytotoxic effects on BC cells by inducing apoptosis

The inhibition of cell growth is accompanied by cell cycle and Annexin V-FITC / PI double staining. Our results showed that PHY treatment increased the proportion of BC cells in the Sub G1 phase, indicating that PHY caused late apoptosis. Moreover, Annexin V-FITC/PI staining assay suggested that PHY could induce BC cell apoptosis after toxic concentration treatments of PHY 30 μg/mL (Fig. 2.2A-B). For the confirmation of the apoptosis induction of PHY on BC cells, we further performed western blot analysis to check the expression levels of apoptosis related proteins (BAX, Bcl-x, PARP and Caspase-3). As shown in Figure 2.2C, PHY reduced protein levels of Bcl-xL while increased protein levels of Bax, cleaved caspase-3 and PARP. Collectively, these results suggest that PHY could inhibit cell growth through the induction of apoptosis in BC cells.

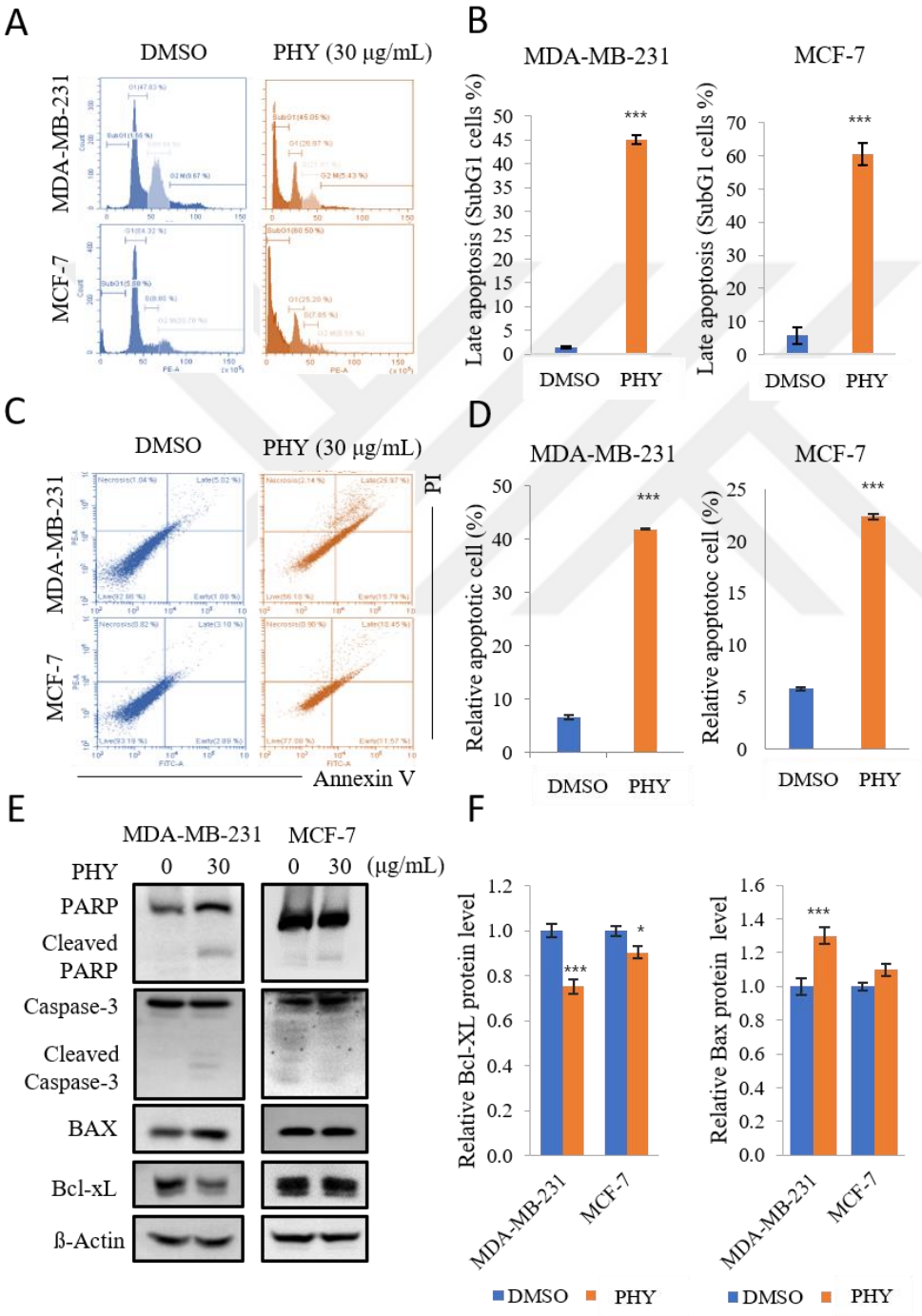
A
DMSO
PHY (30 μg/mL)
MDA-MB-231
MCF-7
B
MDA-MB-231
MCF-7
Late apoptosis (SubG1 cells %)
***
DMSO
PHY
C
DMSO
PHY (30 μg/mL)
MDA-MB-231
MCF-7
PI
Annexin V
D
MDA-MB-231
MCF-7
Relative apoptotic cell (%)
Relative apoptotoc cell (%)
***
DMSO
PHY
E
MDA-MB-231
MCF-7
PHY
0
30
0
30
(μg/mL)
PARP
Cleaved PARP
Caspase-3
Cleaved Caspase-3
BAX
Bcl-xL
ß-Actin
F
Relative Bcl-XL protein level
Relative Bax protein level
***
*
MDA-MB-231
MCF-7
DMSO
PHY

Figure 2.2. PHY induces the apoptosis on BC cells with toxic concentration treatments. BC cells were cultured in the presence of toxic concentrations (30 μg/mL) of PHY for 48 h. (A) Cell cycle analysis was performed by Cytoflex Flow Cytometer (B) Quantitative measurement of late apoptotic cells after detecting Sub-G1 population (C) Cells were stained with Annexin V-FITC/PI to analyze apoptotic and necrotic cell populations by Cytoflex Flow Cytometer. (D) Quantitative results were represented after toxic concentration treatment on the cells. (E) Western blot analysis of the expression of apoptotic proteins PARP, caspase-3, Bax and, Bcl-XL in cells treated with PHY. β-actin served as a loading control. Data represent the mean ± standard error of the mean, n = 3. * $P < 0.05$; *** $P < 0.001$

2.3.3. PHY suppresses motility, proliferation, and tumorigenic potential of BC cells

Cell motility, proliferation and tumor formation are critical actions during cancer development and progression (Gamage et al., 2019). To determine the impact of PHY treatment on the motility of BC cells, scratch wounding migration assay was carried out by the IncuCyte HD system. Non-toxic concentrations of PHY (1.5, 3 and 6 µg/mL) were used for the treatment. As shown in Figure 2.3A, PHY treatment dose dependently decreased the migrated cell numbers in MDA-MB-231 cells. To investigate antiproliferative and anti-tumorigenic potential in vitro, clonogenic (anchorage dependent) and soft agar colony formation (anchorage independent) assay was carried out with PHY on BC cells. As shown in Figure 2.3B and 2.3C, proliferation and tumorigenesis ability of BC cells was significantly reduced by PHY treatment in a dose dependent manner. Taken together, PHY significantly suppresses the motility, proliferation and tumorigenicity of BC cells at non-toxic concentrations.

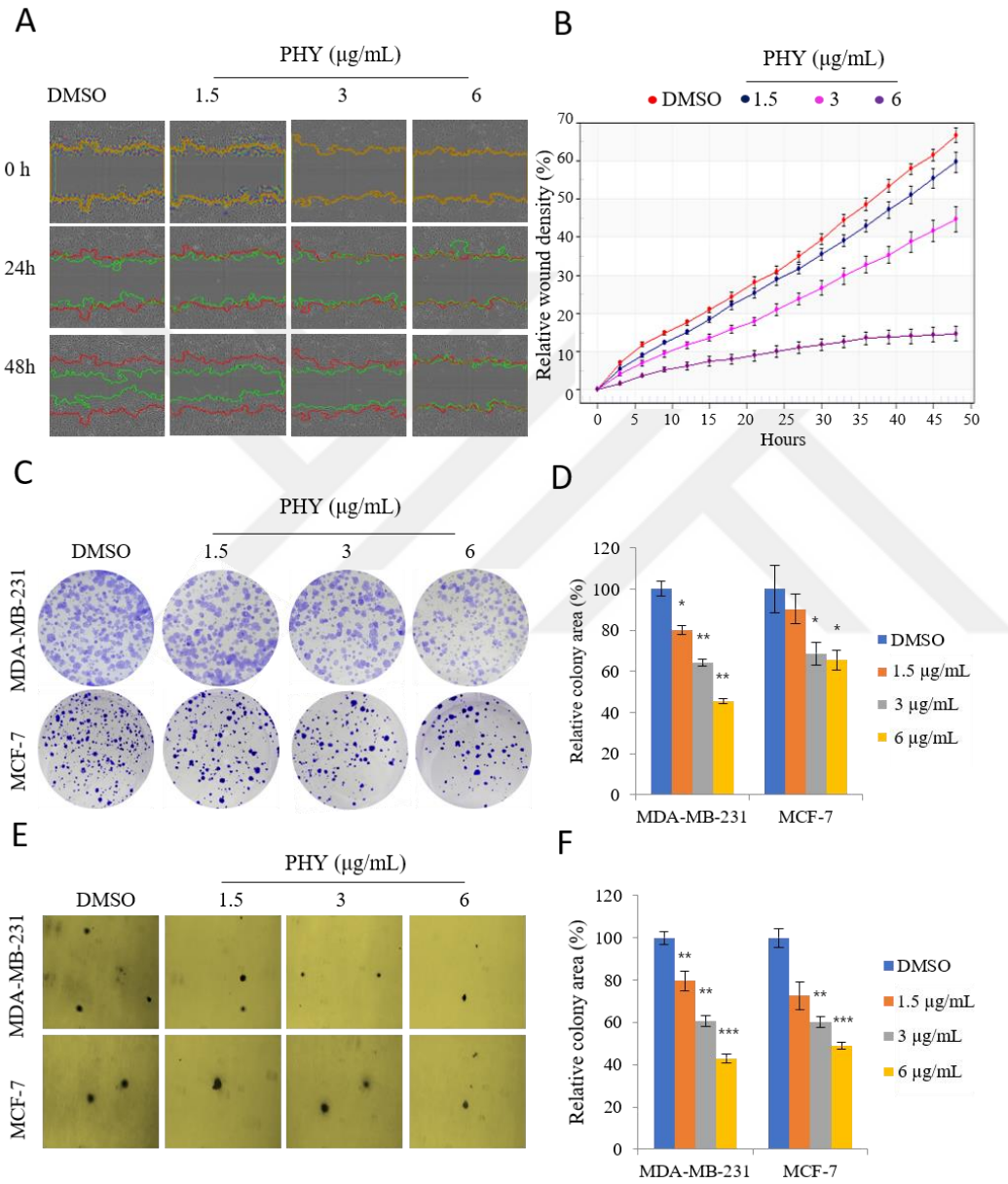
A
PHY (μg/mL)
DMSO
1.5
3
6
0 h
24h
48h
B
PHY (μg/mL)
DMSO
1.5
3
6
Relative wound density (%)
Hours
C
PHY (μg/mL)
DMSO
1.5
3
6
MDA-MB-231
MCF-7
D
Relative colony area (%)
MDA-MB-231
MCF-7
DMSO
1.5 μg/mL
3 μg/mL
6 μg/mL
E
PHY (μg/mL)
DMSO
1.5
3
6
MDA-MB-231
MCF-7
F
Relative colony area (%)
MDA-MB-231
MCF-7
DMSO
1.5 μg/mL
3 μg/mL
6 μg/mL

Figure 2.3. PHY significantly suppresses the motility, proliferation and tumorigenicity of BC cells. To show the effects of PHY on the motility of MBA-MB-231 cells, Scratch wounding migration assay was performed by the IncuCyte HD system. Non-toxic concentrations of PHY (1.5, 3 and 6 µg/mL) were treated for 48 h. (A) Representative images of each wound area. (B) Quantitative data of relative wound density (RWD). (C) Representative images of each well in anchorage dependent clonogenic assay. (D) Quantitative results of the percentage of colony area in each treatment. To determine the anti-tumorigenic potential of PHY, soft agar colony formation assay was performed. 2500 cells/well were seeded into 12 well plate. Once in three days, treated with non-toxic concentration, incubated for 2weeks. (B) Representative images of each PHY treated colonies (B) Quantitative results of the colonies of the BC cells. Data represent the mean ± standard error of the mean, n = 3. * $P < 0.05$; ** $P < 0.01$; *** $P < 0.001$

2.3.4. PHY leads to mitochondrial dysfunction in BC cells

The ability of PHY treatment on BC cells metabolic profile was examined by assessing mitochondrial function by using a Seahorse XFe96 analyzer. Mitochondrial function was assessed through real-time oxidative phosphorylation by monitoring oxygen consumption rate (OCR), and sequentially, injections of oligomycin, FCCP, and an antimycin/rotenone mix allowed us to evaluate mitochondrial function parameters such as basal respiration, maximal respiration, ATP production, proton leak, and spare respiratory capacity. Our results showed a significant reduction of OCR level and all mitochondrial respiration parameters (Fig.2.4A-D). Taken together, our data indicate that PHY treatment disrupts the mitochondrial respiration of BC cells.

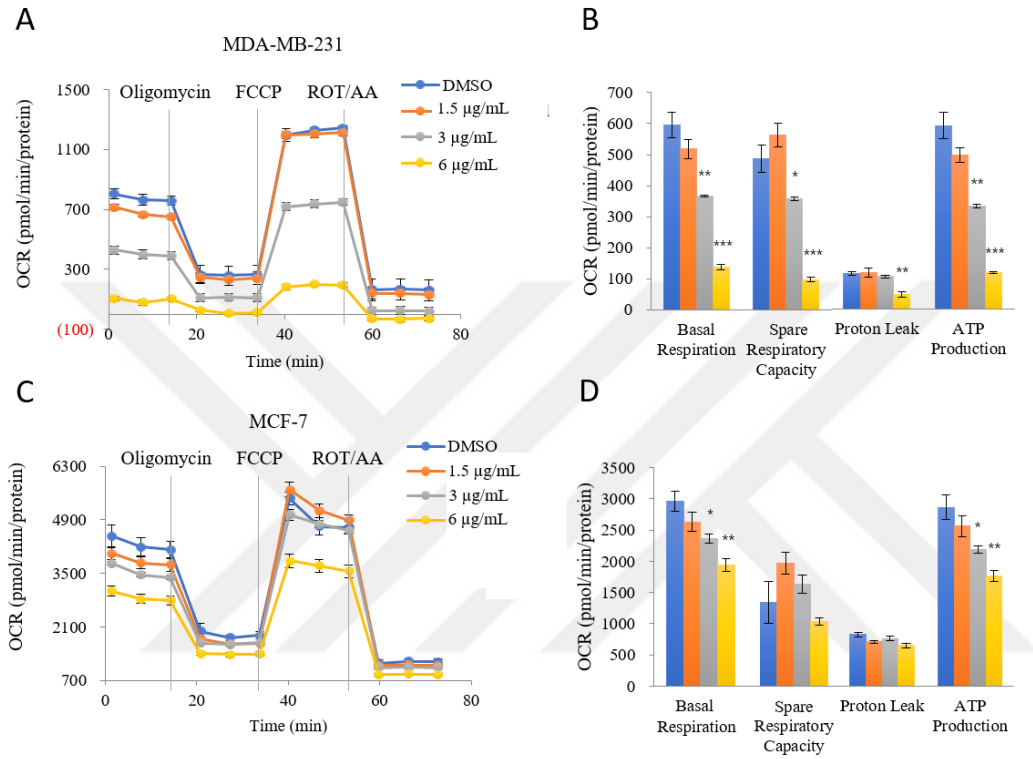

Figure 2.4 PHY induces mitochondrial dysfunction in BC cells**.** BC cells were treated with different concentrations of PHY (1.5, 3, and 6 μg/mL) for 48 h. (A-C) oxygen consumption rate (OCR) were detected by Seahorse XF96 extracellular flux analyzer using the Cell Mito Stress Test Kit. OCR was measured at three time points, followed by sequential injection of oligomycin (1 μM), FCCP (0.5 μM), rotenone (1 μM), and antimycin A (1 μM). Basal respiration, spare respiratory capacity, proton leak, and ATP production were assessed, respectively. Data represent the mean ± standard error of the mean, n = 3. * $P < 0.05$; ** $P < 0.01$; *** $P < 0.001$

2.3.5. PHY suppresses aerobic glycolysis in BC cells

Glycolytic function, known as aerobic glycolysis or Warburg effect, in BC cells was assessed with the extracellular acidification rate (ECAR) by the glycolytic rate assay including antimycin/rotenone mix and 2-deoxy-D-glucose (2-DG). To measure glycolytic rates, Seahorse XF Glycolytic Rate Assay utilizes both ECAR and OCR measurements to determine the glycolytic proton efflux rate (glycoPER) of the cells (Fig. 2.5A-C). As shown in figure 2.5B-D, glycolytic parameters including the basal and compensatory glycolysis significantly decreased in a dose-dependent manner in both BC cells. Taken together, the results showed that aerobic glycolysis was suppressed by PHY treatment in BC cells.

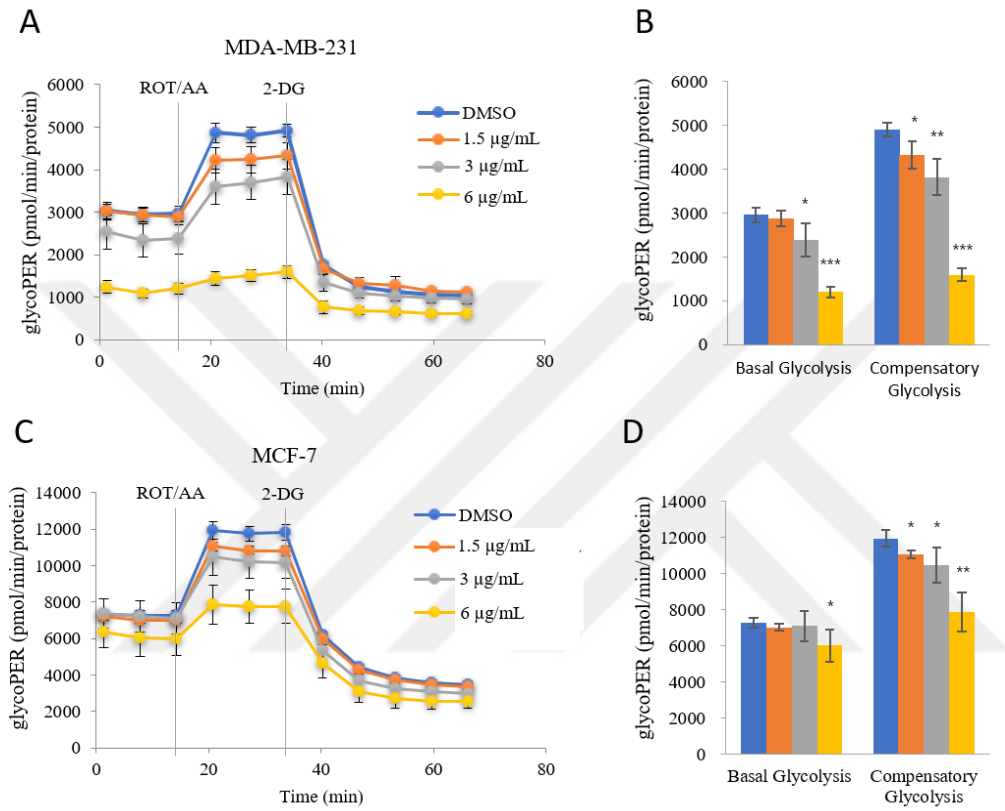

Figure 2.5. PHY suppressed aerobic glycolysis in BC cells**.** PHY inhibited lactate production and glucose uptake in BC cell lines MCF-7 and MDA-MB-231 in a dose-dependent manner. BC cells were treated with different concentrations of PHY (1.5, 3, and 6 µg/mL). (A-D) The extracellular acidification rate (ECAR) and oxygen consumption rate (OCR) were detected by Seahorse XF96 extracellular flux analyzer using the Glycolytc Rate Assay kit. To measure glycolytic rates, Seahorse XF Glycolytic Rate Assay utilizes both ECAR and OCR measurements to determine the glycolytic proton efflux rate (glycoPER) of the cells. glycoPER

was measured at two time points, followed by sequential injection of rotenone (1 μM)/ antimycin A (1 μM) and 2-DG (50 mM). Data represent the mean ± standard error of the mean, n = 3. * $P < 0.05$; ** $P < 0.01$; *** $P < 0.001$

2.3.6. PHY alters glucose metabolism-related gene expressions

To further elucidate how PHY suppresses aerobic glycolysis in BC cells, we examined the expression of several key markers in the regulation of glycolytic pathways including PKM2, Glut1 and LDHA. We observed that mRNA level of Glut1, PKM2, and LDHA were significantly reduced by PHY treatment (Fig.2.6A-B). Moreover, we further confirmed the PHY treatment led to the reduction of these proteins in dose dependent manner (Fig.2.6C-D). These findings suggest that PHY regulates the expression of key enzymes in the glycolytic pathway to suppress aerobic glycolysis in BC cells.

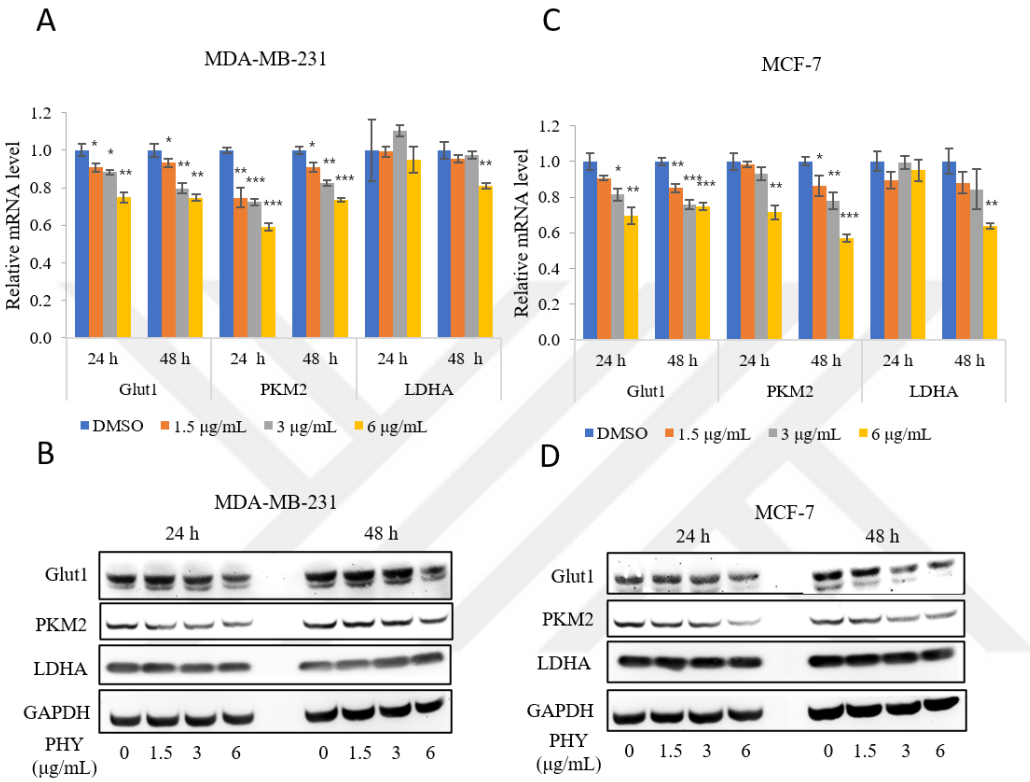

Figure 2.6 PHY suppress glucose metabolism-related gene expressions. To clarify the additional mechanisms whereby PHY modulates cell metabolism, we performed qRT-PCR and western blotting to detect possible target for PHY. (A) Quantitative analysis of the mRNA levels Glut1, PKM2 and LDHA in BC cells with different dosage. (B) Protein levels of tested glycolytic marker in BC cells treated with PHY. Data represent the mean ± standard error of the mean, n = 3. * $P < 0.05$; ** $P < 0.01$; *** $P < 0.001$.

2.3.7. PHY downregulates PKM2 related transcription factors and oncogenes

HIF-1α is a transcription factor which plays critical roles in various stages of carcinogenesis including cell division, glycolytic metabolism, angiogenesis and cell survival (Jun et al., 2017). NF-κB and STAT3 are two major transcriptional factors controlling the ability of pre-neoplastic and malignant cells to resist apoptosis-based tumor-surveillance and regulating tumor angiogenesis and invasiveness (Fan et al., 2013). They also cooperate with HIF-1 to induce the reprogramming tumor glycolysis (Poli and Camporeale, 2015; Rodríguez-Enríquez et al., 2019). Here, figure 2.7 A-B shows that whereas expression of HIF-1α was significantly decreased by PHY treatment, P-NF-κB and P-STAT3 was slightly downregulated. Wnt and its downstream effectors, when deregulated, promote cancer initiation, growth, and metastasis (Tai et al., 2015). Therefore, we then analyzed whether PHY could affect Wnt/β-catenin pathway. Activation of β-catenin also modulates downstream target genes including cyclin D1 and c-Myc, which are involved in tumor cell proliferation (Stewart, 2014). β-catenin transactivation through interaction with PKM2, which plays a critical role in transcription of CCND1 and c-Myc (Yang et al., 2011) . As shown in Figure 6, PHY treatment resulted in decreased β-catenin expression level and its downstream targets cyclin-D1 and c-Myc. Overall, our results suggest that PHY might be regulate growth inhibition and glycolytic metabolism of BC cells through the

PKM2 related transcription factors and oncogenes.

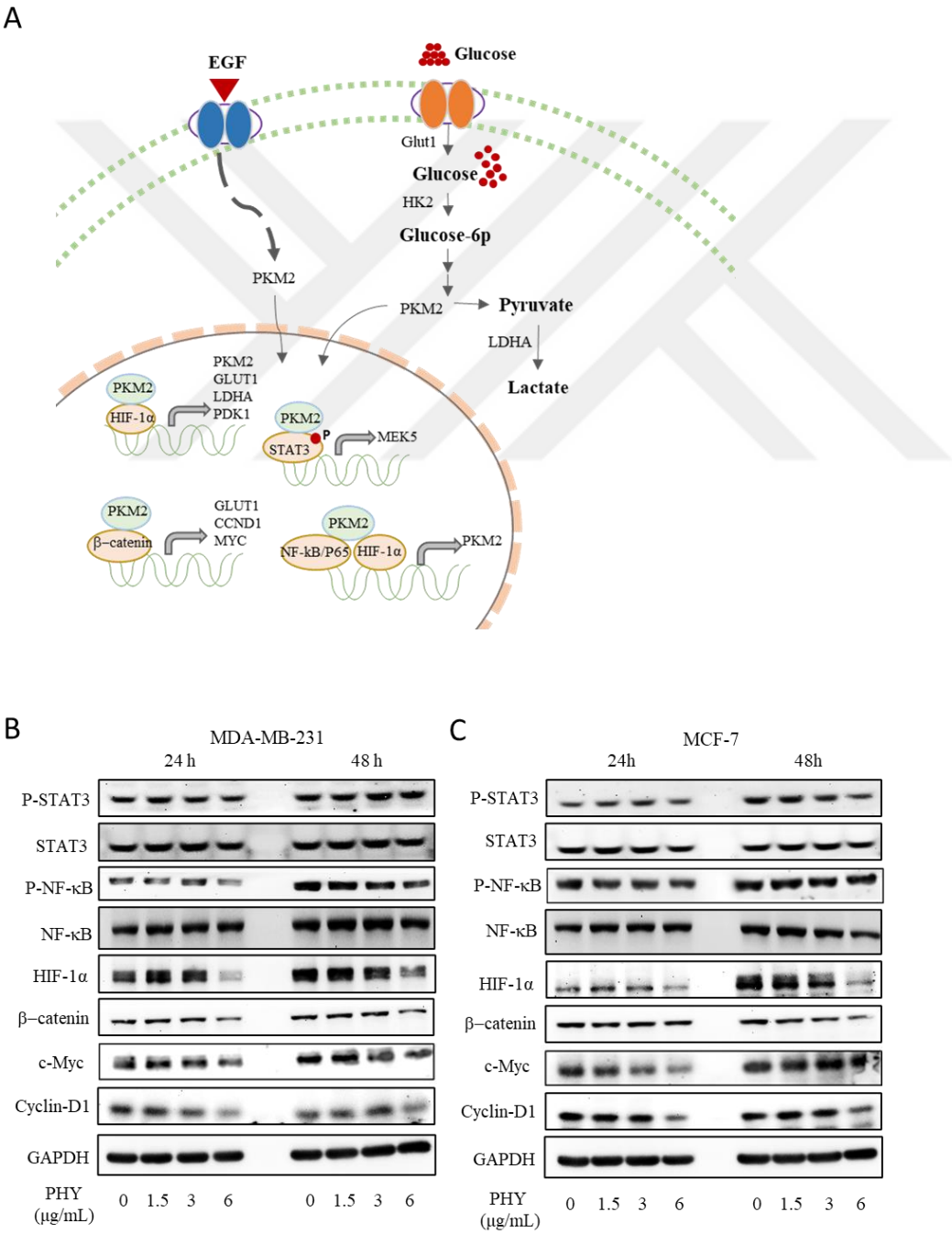

Figure 2.7. PHY downregulates PKM2 related transcription factors and oncogenic targets. (A) Nuclear translocation of PKM2 and interaction with other transcription factors and oncogenes as a transcription factor and a tyrosine kinase. (B-C) The protein levels of P-STAT3, STAT3, P-NF-κB, NF-κB, HIF-1α, β-catenin, c-Myc, and cyclin-D1 were screened by PHY in each BC cells.

2.3.8. PHY suppresses the orthotopic growth of BC *in vivo*

To evaluate the effect of PHY in vivo, 4T1-iRFP inoculated orthotopic mouse model was generated (Fig.2.8A). After 9 days, tumor bearing mice were treated with control (DMSO) and PHY (5 mg/kg body weight) intraperitoneally (i.p) once in 3 days for around 3 weeks. As shown in Figure 2.8, PHY treatment suppressed 30% both tumor volume and weight compared to control group (Fig.2.8C-D). Bioimaging was performed to observe the tumor mass of each mice by FOBI system (Fig.2.8E). PHY did not reduce the body weight of mice, suggesting that it has no toxic effect on mice (Fig.2.8F). Together, these results demonstrated that PHY reduces 4T1-iRFP orthotopic tumor growth.

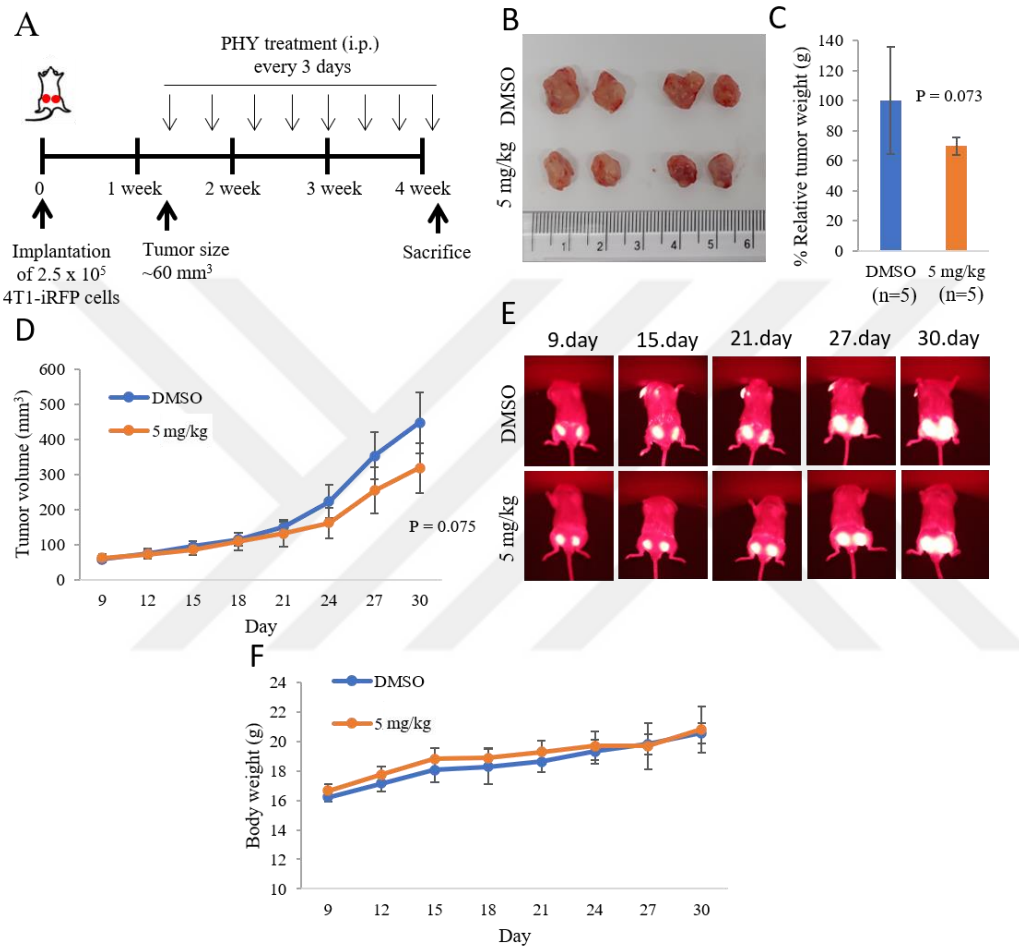
A
PHY treatment (i.p.)
every 3 days
0
1 week
2 week
3 week
4 week
Implantation
of 2.5 x 10^5
4T1-iRFP cells
Tumor size
~60 mm^3
Sacrifice
B
DMSO
5 mg/kg
C
% Relative tumor weight (g)
P = 0.073
DMSO
(n=5)
5 mg/kg
(n=5)
D
Tumor volume (mm^3)
DMSO
5 mg/kg
P = 0.075
Day
E
9.day
15.day
21.day
27.day
30.day
DMSO
5 mg/kg
F
Body weight (g)
DMSO
5 mg/kg
Day

Figure 2.8. PHY reduced orthotopic 4T1-iRFP tumor growth in vivo. 4T1-iRFP cells (2.5×10^5) injected into mammary fat pads of the BALB/c mice (n=10). 9 days after cell implantation, PHY treatment (5 mg/kg body weight injected intraperitoneally (i.p.) once in 3 days) started and continued around 3 weeks. (A) Schedule of in vivo experiment with 4T1-iRFP cells. (B) Representative photograph of xenograft tumors collected from sacrificed mice at the end of treatment period. (C) Average tumor weight of resected tumors from mice. (D) Tumor volumes recorded at injection times in mice. (E) Bioimaging pictures performed by fluorescence-labeled organism bioimaging instrument (FOBI) system. (F) Body weight of mice treated with control and PHY.

2.4. Discussion

Breast cancer (BC) represents one-fourth of all cancer cases and the most common cancer diagnosed in women. Although a decline in BC mortality has been observed over the last 40 years, incidence continues to rise, particularly in developing countries (Abrahams et al., 2016; DeSantis et al., 2017). In general, patients with estrogen receptor–positive (ER+) breast cancer receive adjuvant endocrine therapy in addition to chemotherapy in advanced cases; patients with human epidermal growth factor receptor 2–positive (HER2+) breast cancer often receive anti-HER2 therapy combined with chemotherapy; and patients with triple-negative breast cancer (TNBC) receive chemotherapy (Senkus et al., 2013).

Lichens are symbiotic organisms that synthesise bioactive metabolites with a variety of effects (Zhou et al., 2017). PHY is an effective metabolite isolated from the Chile lichen *Pseudocyphellaria* sp. We previously reported that PHY has anti-metastatic, anti-proliferative and anti-tumor activity on colorectal and lung cancer cells with molecular mechanism of action (Taş et al., 2019a; Yang et al., 2015). Here, we investigated the effects of PHY on growth, and metabolism of BC cells. we found the followings: 1) PHY decreases BC cell viability through inducing apoptosis at toxic concentration; 2) PHY suppresses motility, proliferation, and tumorigenic potential of BC cells *in vitro*; 3) PHY leads to mitochondrial dysfunction and suppresses aerobic glycolysis in BC cells; 4) PHY alters glucose

metabolism-related gene expressions; 5) PHY downregulates PKM2 related transcription factors and oncogenes and 6) PHY suppresses the orthotopic growth of BC *in vivo* without showing toxicity features at tested dosage. Collectively, through this study, we provide the therapeutic potential of PHY on the growth of BC cells.

Cancer cells exhibit altered nutrient acquisition and metabolic pathways, to keep up with the bioenergetic, biosynthetic and reduction-oxidation (REDOX) needs of a rapidly dividing tumor. This phenomenon has been identified as a hallmark of cancer, leading to a growing interest in the exploitation of cancer cell metabolism (CCM) in cancer therapeutics. The 'Warburg Effect' of aerobic glycolysis, posited defective mitochondrial-based oxidative phosphorylation (OXPHOS) leading to a metabolic switch in cancer cells towards glycolytic pathways, irrespective of oxygen tension. (Ngoi et al., 2020).

Cellular metabolism plays an integral role in numerous biological processes, and investigation into cancer metabolism can greatly enhance our understanding of cancer biology. The discovery of cancer-associated mutations in genes encoding key metabolic enzymes has provided a direct link between altered metabolism and cancer (Ogrodzinski et al., 2017; Yang et al., 2013). Altered metabolic activity is crucial for supporting uncontrolled proliferation, evasion of growth-inhibitory signals, cell migration and the dissemination of metastatic cells into distant tissues.

However, metabolic reprogramming also renders cancer cells more susceptible to perturbations within the metabolic network (Schulze and Harris, 2012).

ER+ BC cell, MCF-7, is associated with a more favorable prognosis than HER2+, progesterone receptor-positive (PR+), and TNBC. Although anti-estrogen therapy using tamoxifen is an effective way to treat some ER+ breast tumors, treatment of 66% of ER+/PR−, 55% of ER−/PR+, and 25% of ER+/PR+ breast cancer patients fails (Deblois and Giguère, 2013). Moreover, due to the lack of ER, PR, and HER2 expression in TNBC cells targeted therapies are currently unavailable. Thus, developing new therapeutic targets based on metabolic vulnerabilities is especially promising for improving BC patient outcomes (Deblois and Giguère, 2013; Kim et al., 2013; Ogrodzinski et al., 2017).

It is intriguing that a glycolytic enzyme, PKM2, can function as a protein kinase or a trans-activator and translocate to the nucleus acting on gene transcription. Thus, PKM2 affects a variety of signaling pathways to promote tumor development (Gao et al., 2012; Zhang et al., 2019). PKM2 functions as a coactivator that stimulates HIF-1 transactivation of target genes encoding GLUT1, LDHA, and PDK1 in cancer cells. PKM2 participates in a positive feedback loop that promotes HIF-1 transactivation and reprograms glucose metabolism in cancer cells (Luo et al., 2011). PKM2 contributes to tumor growth and angiogenesis by regulating HIF-1α via NF-κB activation. Hypoxic insult is

followed by translocation of PKM2 and p65 to the nucleus in pancreatic cancer cells. Following the interaction with PKM2, NF-κB subunit p65 activates the transcription of HIF-1α and its target gene VEGF-A. As a result, augmented secretion of VEGF translates to a boost in blood vessel formation, which in turn contributes to tumor growth (Azoitei et al., 2016). Here, we showed the PHY suppresses the expression of NF-κB and HIF-1α along with PKM2 suggesting that it might be possible mechanism behind the suppression of aerobic glycolysis.

The WNT is an essential signaling pathway for numerous biological processes including embryogenesis, modulation of cell cycle, inflammatory changes, and cancer (Tai et al. 2015). The Wnt signaling pathways are subdivided into the canonical β-catenin-dependent pathway and the noncanonical β-catenin-independent pathway (Novellasdemunt et al. 2015). c-Myc is a pivotal target of β-catenin and regulates thousands of genes. Aberrantly high expression of c-Myc is a common basis of tumorigenesis and c-Myc is also a key oncogenic driver of glycolysis in normoxia. Downregulation the expression and nuclear translocation of β-catenin, followed by suppression of c-Myc and downstream glycolytic genes of GLUT1, LDHA, HK2, and PKM2 in several cancer cells, which led to decreased glycolytic activity (Fang et al., 2019). Our results showed that PHY has potential to suppress β-catenin and its downstream genes c-Myc and cyclin-D1, suggesting

that these might be possible underlying mechanism of anti-tumor activity as well as suppression of aerobic glycolysis (Fig.2.7).

JAK2 and c-Src are the most common protein tyrosine kinases that phosphorylate STAT3. Moreover, it was reported that PKM2 increased the STAT3 binding to its target sequence both in vitro and in vivo and showed that PKM2 plays a role in STAT3 phosphorylation at Y705 (Gao et al., 2012). Activation of STAT3 represents probably one of the most important molecular signatures involved in promoting cancer progression. It has been observed that activation of STAT3 is detected in almost all cancer types (Gao et al., 2012; Groner et al., 2008; Taş et al., 2019b). Here, we exhibited the PHY reduces the expression of STAT3 along with PKM2 suggesting that it might be possible mechanism behind the suppression of cell proliferation and tumorigenesis.

Because PHY treatment suppressed the growth of BC cell in vitro conditions, our last objective was to confirm in vitro results in orthotopic mouse model of BC. Our results showed that PHY (5 mg/kg body weight) inhibited orthotopic growth of 4T1-iRFP cell in mice. In addition, there was no reduction in body weight among the control and PHY treated groups. These findings clearly indicate that PHY has potential activity against BC orthotopic model without toxic effect. In summary, the findings from our cell-based *in vitro* and *in vivo* researches

support the antiproliferative, apoptosis induction, suppression of cell energy metabolism and tumorigenesis activity of PHY.

Conclusion

In conclusion, our findings indicated that PHY showed significant anticancer activities against BC and CRC cell lines in vitro. Furthermore, PHY inhibited tumor growth in orthotopic and skin xenograft mouse models. Collectively, these results suggest that PHY has a potential further in vivo application as an anti-proliferative, anti-glycolytic and anti-tumorigenic agent.

References

Abrahams, H.J.G., Gielissen, M.F.M., Schmits, I.C., Verhagen, C.A.H.H.V.M., Rovers, M.M., Knoop, H., 2016. Risk factors, prevalence, and course of severe fatigue after breast cancer treatment: A meta-analysis involving 12 327 breast cancer survivors. Ann. Oncol. 27, 965–974. https://doi.org/10.1093/annonc/mdw099

Azoitei, N., Becher, A., Steinestel, K., Rouhi, A., Diepold, K., Genze, F., Simmet, T., Seufferlein, T., 2016. PKM2 promotes tumor angiogenesis by regulating HIF-1aα through NF-κB activation. Mol. Cancer 15, 3. https://doi.org/10.1186/s12943-015-0490-2

Cao, H., Xu, E., Liu, H., Wan, L., Lai, M., 2015. Epithelial–mesenchymal transition in colorectal cancer metastasis: A system review. Pathol. - Res. Pract. 211, 557–569. https://doi.org/10.1016/J.PRP.2015.05.010

Chaitanya, G., Alexander, J.S., Babu, P., 2010. PARP-1 cleavage fragments: signatures of cell-death proteases in neurodegeneration. Cell Commun. Signal. 8, 31. https://doi.org/10.1186/1478-811X-8-31

Crawford, S.D., 2015. Lichens Used in Traditional Medicine, in: Lichen Secondary Metabolites. Springer International Publishing, Cham, pp. 27–80. https://doi.org/10.1007/978-3-319-13374-4_2

Crowley, L.C., Marfell, B.J., Scott, A.P., Waterhouse, N.J., 2016a. Quantitation of Apoptosis and Necrosis by Annexin V Binding, Propidium Iodide Uptake, and Flow Cytometry. Cold Spring Harb. Protoc. 2016, pdb.prot087288. https://doi.org/10.1101/pdb.prot087288

Crowley, L.C., Marfell, B.J., Waterhouse, N.J., 2016b. Analyzing Cell Death by Nuclear Staining with Hoechst 33342. Cold Spring Harb. Protoc. 2016, pdb.prot087205. https://doi.org/10.1101/pdb.prot087205

Deblois, G., Giguère, V., 2013. Oestrogen-related receptors in breast cancer: Control of cellular metabolism and beyond. Nat. Rev. Cancer 13, 27–36. https://doi.org/10.1038/nrc3396

DeSantis, C.E., Ma, J., Goding Sauer, A., Newman, L.A., Jemal, A., 2017. Breast cancer statistics, 2017, racial disparity in mortality by state. CA. Cancer J. Clin. 67, 439–448. https://doi.org/10.3322/caac.21412

Fan, Y., Mao, R., Yang, J., 2013. NF-κB and STAT3 signaling pathways collaboratively link inflammation to cancer. Protein Cell 4, 176–185. https://doi.org/10.1007/s13238-013-2084-3

Fang, Y., Shen, Z.Y., Zhan, Y.Z., Feng, X.C., Chen, K.L., Li, Y.S., Deng, H.J., Pan, S.M., Wu, D.H., Ding, Y., 2019. CD36 inhibits β-catenin/c-myc-mediated glycolysis through ubiquitination of GPC4 to repress colorectal

tumorigenesis. Nat. Commun. 10, 1–16. https://doi.org/10.1038/s41467-019-11662-3

Ferlay, J., Soerjomataram, I., Dikshit, R., Eser, S., Mathers, C., Rebelo, M., Parkin, D.M., Forman, D., Bray, F., 2015. Cancer incidence and mortality worldwide: Sources, methods and major patterns in GLOBOCAN 2012. Int. J. Cancer 136, E359–E386. https://doi.org/10.1002/ijc.29210

Gamage, C.D.B., Park, S.Y., Yang, Y., Zhou, R., Taş, İ., Bae, W.K., Kim, K.K., Shim, J.H., Kim, E., Yoon, G., Kim, H., 2019. Deoxypodophyllotoxin exerts anti-cancer effects on colorectal cancer cells through induction of apoptosis and suppression of tumorigenesis. Int. J. Mol. Sci. 20. https://doi.org/10.3390/ijms20112612

Gao, X., Wang, H., Yang, J.J., Liu, X., Liu, Z.R., 2012. Pyruvate Kinase M2 Regulates Gene Transcription by Acting as a Protein Kinase. Mol. Cell 45, 598–609. https://doi.org/10.1016/j.molcel.2012.01.001

Graupera, M., Guillermet-Guibert, J., Foukas, L.C., Phng, L.-K., Cain, R.J., Salpekar, A., Pearce, W., Meek, S., Millan, J., Cutillas, P.R., Smith, A.J.H., Ridley, A.J., Ruhrberg, C., Gerhardt, H., Vanhaesebroeck, B., 2008. Angiogenesis selectively requires the p110α isoform of PI3K to control endothelial cell migration. Nature 453, 662–666.

https://doi.org/10.1038/nature06892

Groner, B., Lucks, P., Borghouts, C., 2008. The function of Stat3 in tumor cells and their microenvironment. Semin. Cell Dev. Biol. https://doi.org/10.1016/j.semcdb.2008.06.005

Gulhati, P., Bowen, K.A., Liu, J., Stevens, P.D., Rychahou, P.G., Chen, M., Lee, E.Y., Weiss, H.L., O'Connor, K.L., Gao, T., Evers, B.M., 2011. mTORC1 and mTORC2 regulate EMT, motility, and metastasis of colorectal cancer via RhoA and Rac1 signaling pathways. Cancer Res. 71, 3246–56. https://doi.org/10.1158/0008-5472.CAN-10-4058

Hanna, S., El-Sibai, M., 2013. Signaling networks of Rho GTPases in cell motility. Cell. Signal. 25, 1955–1961. https://doi.org/10.1016/J.CELLSIG.2013.04.009

Hu, Y., Yu, K., Wang, G., Zhang, Depeng, Shi, C., Ding, Y., Hong, D., Zhang, Dan, He, H., Sun, L., Zheng, J.-N., Sun, S., Qian, F., 2018. Lanatoside C inhibits cell proliferation and induces apoptosis through attenuating Wnt/β-catenin/c-Myc signaling pathway in human gastric cancer cell. Biochem. Pharmacol. 150, 280–292. https://doi.org/10.1016/J.BCP.2018.02.023

Huneck, S., Yoshimura, I., 1996. Identification of Lichen Substances, in: Identification of Lichen Substances. Springer Berlin Heidelberg, Berlin,

Heidelberg, pp. 11–123. https://doi.org/10.1007/978-3-642-85243-5_2

Jang, M., Kim, S.S., Lee, J., 2013. Cancer cell metabolism: Implications for therapeutic targets. Exp. Mol. Med. 45, e45–e45. https://doi.org/10.1038/emm.2013.85

Jun, J.C., Rathore, A., Younas, H., Gilkes, D., Polotsky, V.Y., 2017. Hypoxia-Inducible Factors and Cancer. Curr. Sleep Med. Reports 3, 1–10. https://doi.org/10.1007/s40675-017-0062-7

Kim, M.K., Park, G.H., Eo, H.J., Song, H.M., Lee, J.W., Kwon, M.J., Koo, J.S., Jeong, J.B., 2015. Tanshinone I induces cyclin D1 proteasomal degradation in an ERK1/2 dependent way in human colorectal cancer cells. Fitoterapia 101, 162–168. https://doi.org/10.1016/J.FITOTE.2015.01.010

Kim, S., Kim, D.H., Jung, W.H., Koo, J.S., 2013. Metabolic phenotypes in triple-negative breast cancer. Tumor Biol. 34, 1699–1712. https://doi.org/10.1007/s13277-013-0707-1

Komorowski, A.S., Warner, E., MacKay, H.J., Sahgal, A., Pritchard, K.I., Jerzak, K.J., 2020. Incidence of Brain Metastases in Nonmetastatic and Metastatic Breast Cancer: Is There a Role for Screening? Clin. Breast Cancer. https://doi.org/10.1016/j.clbc.2019.06.007

Koopman, G., Reutelingsperger, C.P., Kuijten, G.A., Keehnen, R.M., Pals, S.T.,

van Oers, M.H., 1994. Annexin V for flow cytometric detection of phosphatidylserine expression on B cells undergoing apoptosis. Blood 84, 1415–20.

Kurisu, S., Takenawa, T., 2010. WASP and WAVE family proteins: Friends or foes in cancer invasion? Cancer Sci. 101, 2093–2104. https://doi.org/10.1111/j.1349-7006.2010.01654.x

Lee, H., Cho, H., Yu, R., Lee, K., Chun, H., Park, J., 2014. Mechanisms Underlying Apoptosis-Inducing Effects of Kaempferol in HT-29 Human Colon Cancer Cells. Int. J. Mol. Sci. 15, 2722–2737. https://doi.org/10.3390/ijms15022722

Lee, J.H., Park, S.R., Chay, K.-O., Seo, Y.-W., Kook, H., Ahn, K.Y., Kim, Y.J., Kim, K.K., 2004. KAI1 COOH-terminal interacting tetraspanin (KITENIN), a member of the tetraspanin family, interacts with KAI1, a tumor metastasis suppressor, and enhances metastasis of cancer. Cancer Res. 64, 4235–43. https://doi.org/10.1158/0008-5472.CAN-04-0275

Lee, S., Song, Y.-A., Park, Y.-L., Cho, S.-B., Lee, W.-S., Lee, J.-H., Chung, I.-J., Kim, K.-K., Rew, J.-S., Joo, Y.-E., 2011. Expression of KITENIN in human colorectal cancer and its relation to tumor behavior and progression. Pathol. Int. 61, 210–220. https://doi.org/10.1111/j.1440-1827.2011.02646.x

Li, S., Kuo, H.C.D., Yin, R., Wu, R., Liu, X., Wang, L., Hudlikar, R., Peter, R.M.,

Kong, A.N., 2020. Epigenetics/epigenomics of triterpenoids in cancer prevention and in health. Biochem. Pharmacol. https://doi.org/10.1016/j.bcp.2020.113890

Luo, W., Hu, H., Chang, R., Zhong, J., Knabel, M., O'Meally, R., Cole, R.N., Pandey, A., Semenza, G.L., 2011. Pyruvate kinase M2 is a PHD3-stimulated coactivator for hypoxia-inducible factor 1. Cell 145, 732–744. https://doi.org/10.1016/j.cell.2011.03.054

Maurer, C.A., Graber, H.U., Friess, H., Beyermann, B., Willi, D., Netzer, P., Zimmermann, A., Büchler, M.W., 1999. Reduced expression of the metastasis suppressor gene KAI1 in advanced colon cancer and its metastases. Surgery 126, 869–80. https://doi.org/10.1016/S0039-6060(99)70028-0

Mazo, C., Kearns, C., Mooney, C., Gallagher, W.M., 2020. Clinical decision support systems in breast cancer: A systematic review. Cancers (Basel). 12, 1–15. https://doi.org/10.3390/cancers12020369

Miller, J., Dreyer, T.F., Bächer, A.S., Sinner, E.-K., Heinrich, C., Benge, A., Gross, E., Preis, S., Rother, J., Roberts, A., Nelles, G., Miteva, T., Reuning, U., 2018. Differential tumor biological role of the tumor suppressor KAI1 and its splice variant in human breast cancer cells. Oncotarget 9, 6369–6390. https://doi.org/10.18632/oncotarget.23968

Nash, T.H., 2008. Lichen Biology, second edition, Lichen Biology, Second Edition. https://doi.org/10.1017/CBO9780511790478

Ngoi, N.Y.L., Eu, J.Q., Hirpara, J., Wang, L., Lim, J.S.J., Lee, S.C., Lim, Y.C., Pervaiz, S., Goh, B.C., Wong, A.L.A., 2020. Targeting Cell Metabolism as Cancer Therapy. Antioxidants Redox Signal. 32, 285–308. https://doi.org/10.1089/ars.2019.7947

Novellasdemunt, L., Antas, P., Li, V.S.W., 2015. Targeting Wnt signaling in colorectal cancer. A Review in the Theme: Cell Signaling: Proteins, Pathways and Mechanisms. Am. J. Physiol. Physiol. 309, C511–C521. https://doi.org/10.1152/ajpcell.00117.2015

Ogrodzinski, M.P., Bernard, J.J., Lunt, S.Y., 2017. Deciphering metabolic rewiring in breast cancer subtypes. Transl. Res. https://doi.org/10.1016/j.trsl.2017.07.004

Poli, V., Camporeale, A., 2015. STAT3-mediated metabolic reprograming in cellular transformation and implications for drug resistance. Front. Oncol. https://doi.org/10.3389/fonc.2015.00121

Qi, J., Yu, Y., Akilli Öztürk, Ö., Holland, J.D., Besser, D., Fritzmann, J., Wulf-Goldenberg, A., Eckert, K., Fichtner, I., Birchmeier, W., 2016. New Wnt/β-catenin target genes promote experimental metastasis and migration of

colorectal cancer cells through different signals. Gut 65, 1690–701. https://doi.org/10.1136/gutjnl-2014-307900

Rodríguez-Enríquez, S., Marín-Hernández, Á., Gallardo-Pérez, J.C., Pacheco-Velázquez, S.C., Belmont-Díaz, J.A., Robledo-Cadena, D.X., Vargas-Navarro, J.L., Corona de la Peña, N.A., Saavedra, E., Moreno-Sánchez, R., 2019. Transcriptional Regulation of Energy Metabolism in Cancer Cells. Cells 8, 1225. https://doi.org/10.3390/cells8101225

Rousseau, S., Houle, F., Kotanides, H., Witte, L., Waltenberger, J., Landry, J., Huot, J., 2000. Vascular endothelial growth factor (VEGF)-driven actin-based motility is mediated by VEGFR2 and requires concerted activation of stress-activated protein kinase 2 (SAPK2/p38) and geldanamycin-sensitive phosphorylation of focal adhesion kinase. J. Biol. Chem. 275, 10661–72. https://doi.org/10.1074/JBC.275.14.10661

Schulze, A., Harris, A.L., 2012. How cancer metabolism is tuned for proliferation and vulnerable to disruption. Nature. https://doi.org/10.1038/nature11706

Sebio, A., Kahn, M., Lenz, H.-J., 2014. The potential of targeting Wnt/β-catenin in colon cancer. Expert Opin. Ther. Targets 18, 611–615. https://doi.org/10.1517/14728222.2014.906580

Senkus, E., Kyriakides, S., Penault-Llorca, F., Poortmans, P., Thompson, A.,

Zackrisson, S., Cardoso, F., 2013. Primary breast cancer: ESMO clinical practice guidelines for diagnosis, treatment and follow-up. Ann. Oncol. 24, vi7–vi23. https://doi.org/10.1093/annonc/mdt284

Sikander, M., Hafeez, B. Bin, Malik, S., Alsayari, A., Halaweish, F.T., Yallapu, M.M., Chauhan, S.C., Jaggi, M., 2016. Cucurbitacin D exhibits potent anti-cancer activity in cervical cancer. Sci. Rep. 6, 36594. https://doi.org/10.1038/srep36594

Stewart, D.J., 2014. Wnt Signaling Pathway in Non-Small Cell Lung Cancer. JNCI J. Natl. Cancer Inst. 106, djt356–djt356. https://doi.org/10.1093/jnci/djt356

Tai, D., Wells, K., Arcaroli, J., Vanderbilt, C., Aisner, D.L., Messersmith, W.A., Lieu, C.H., 2015. Targeting the WNT Signaling Pathway in Cancer Therapeutics. Oncologist 20, 1189–98. https://doi.org/10.1634/theoncologist.2015-0057

Taş, İ., Han, J., Park, S.-Y., Yang, Y., Zhou, R., Gamage, C.D.B., Van Nguyen, T., Lee, J.-Y., Choi, Y.J., Yu, Y.H., Moon, K.-S., Kim, K.K., Ha, H.-H., Kim, S.K., Hur, J.-S., Kim, H., 2019a. Physciosporin suppresses the proliferation, motility and tumourigenesis of colorectal cancer cells. Phytomedicine. https://doi.org/10.1016/j.phymed.2018.09.219

Tas, I., Yildirim, A.B., Ozkan, E., Ozyigitoglu, G.C., Yavuz, M.Z., Turker, A.U.,

2019. Biological evaluation and phytochemical profiling of some lichen species. Acta Aliment. 48, 457–465. https://doi.org/10.1556/066.2019.48.4.7

Taş, İ., Zhou, R., Park, S.-Y., Yang, Y., Gamage, C.D.B., Son, Y.-J., Paik, M.-J., Kim, H., 2019b. Inflammatory and tumorigenic effects of environmental pollutants found in particulate matter on lung epithelial cells. Toxicol. Vitr. 59, 300–311. https://doi.org/10.1016/J.TIV.2019.05.022

Tögel, L., Nightingale, R., Chueh, A.C., Jayachandran, A., Tran, H., Phesse, T., Wu, R., Sieber, O.M., Arango, D., Dhillon, A.S., Dawson, M.A., Diez-Dacal, B., Gahman, T.C., Filippakopoulos, P., Shiau, A.K., Mariadason, J.M., 2016. Dual Targeting of Bromodomain and Extraterminal Domain Proteins, and WNT or MAPK Signaling, Inhibits c-MYC Expression and Proliferation of Colorectal Cancer Cells. Mol. Cancer Ther. 15, 1217–26. https://doi.org/10.1158/1535-7163.MCT-15-0724

Vernieri, C., Casola, S., Foiani, M., Pietrantonio, F., de Braud, F., Longo, V., 2016. Targeting cancer metabolism: Dietary and pharmacologic interventions. Cancer Discov. 6, 1315–1333. https://doi.org/10.1158/2159-8290.CD-16-0615

Vu, T., Datta, P., 2017. Regulation of EMT in Colorectal Cancer: A Culprit in Metastasis. Cancers (Basel). 9, 171. https://doi.org/10.3390/cancers9120171

Woolf, E.C., Syed, N., Scheck, A.C., 2016. Tumor metabolism, the ketogenic diet and β-hydroxybutyrate: Novel approaches to adjuvant brain tumor therapy. Front. Mol. Neurosci. 9, 122. https://doi.org/10.3389/fnmol.2016.00122

Yang, M., Soga, T., Pollard, P.J., 2013. Oncometabolites: Linking altered metabolism with cancer. J. Clin. Invest. https://doi.org/10.1172/JCI67228

Yang, W., Xia, Y., Ji, H., Zheng, Y., Liang, J., Huang, W., Gao, X., Aldape, K., Lu, Z., 2011. Nuclear PKM2 regulates β-catenin transactivation upon EGFR activation. Nature 480, 118–122. https://doi.org/10.1038/nature10598

Yang, Y., Bae, W.K., Lee, J.-Y., Choi, Y.J., Lee, K.H., Park, M.-S., Yu, Y.H., Park, S.-Y., Zhou, R., Taş, İ., Gamage, C., Paik, M.-J., Lee, J.H., Chung, I.J., Kim, K.K., Hur, J.-S., Kim, S.K., Ha, H.-H., Kim, H., 2018a. Potassium usnate, a water-soluble usnic acid salt, shows enhanced bioavailability and inhibits invasion and metastasis in colorectal cancer. Sci. Rep. 8, 16234. https://doi.org/10.1038/s41598-018-34709-9

Yang, Y., Bhosle, S.R., Yu, Y.H., Park, S.Y., Zhou, R., Taş, I., Gamage, C.D.B., Kim, K.K., Pereira, I., Hur, J.S., Ha, H.H., Kim, H., 2018b. Tumidulin, a lichen secondary metabolite, decreases the stemness potential of colorectal cancer cells. Molecules 23. https://doi.org/10.3390/molecules23112968

Yang, Y., Park, S.-Y., Nguyen, T.T., Yu, Y.H., Nguyen, T. Van, Sun, E.G., Udeni,

J., Jeong, M.-H., Pereira, I., Moon, C., Ha, H.-H., Kim, K.K., Hur, J.-S., Kim, H., 2015. Lichen Secondary Metabolite, Physciosporin, Inhibits Lung Cancer Cell Motility. PLoS One 10, e0137889. https://doi.org/10.1371/journal.pone.0137889

Yu, X., Li, S., 2017. Non-metabolic functions of glycolytic enzymes in tumorigenesis. Oncogene 36, 2629–2636. https://doi.org/10.1038/onc.2016.410

Zhang, Y.B., Pan, X.F., Chen, J., Cao, A., Zhang, Y.G., Xia, L., Wang, J., Li, H., Liu, G., Pan, A., 2020. Combined lifestyle factors, incident cancer, and cancer mortality: a systematic review and meta-analysis of prospective cohort studies. Br. J. Cancer 122, 1085–1093. https://doi.org/10.1038/s41416-020-0741-x

Zhang, Z., Deng, X., Liu, Yahui, Liu, Yuanda, Sun, L., Chen, F., 2019. PKM2, function and expression and regulation. Cell Biosci. https://doi.org/10.1186/s13578-019-0317-8

Zhou, R., Yang, Y., Park, S.-Y., Nguyen, T.T., Seo, Y.-W., Lee, K.H., Lee, J.H., Kim, K.K., Hur, J.-S., Kim, H., 2017. The lichen secondary metabolite atranorin suppresses lung cancer cell motility and tumorigenesis. Sci. Rep. 7, 8136. https://doi.org/10.1038/s41598-017-08225-1

Acknowledgement

I would like to express my special regards to my supervisor Jae-Seoun Hur for his dedicated support and guidance. I deeply appreciated for giving me opportunity to have my PhD in Suncheon National University. I am indebted to express my special thanks to my co-supervisor Prof. Hangun Kim for his guidance, support, and patience during my PhD. Thank you also the members of the review committee – Prof. Kyung Keun Kim, Prof. Hyung-Ho Ha and Prof. Man-Jeong Paik, who gave me insightful and helpful comments to improve my thesis.

I warmly express sincere thanks to my MSc supervisor, Prof. Arzu Türker, and Prof. Hakan Türker from department of biology, Bolu Abant Izzet Baysal University of Turkey for supporting and encouraging me to have my PhD degree in Republic of Korea. Also, I would like to give my special thanks to my high school teachers- Hülya Kurt and Nimet Yılmaz İnceoğlu for their encouragement in my education life.

My sincere thanks to my colleagues at the molecular pathophysiology lab in college of pharmacy, Dr. So-Yeon Park, Dr. Yi Yang, Dr. Zhou Rui, Dr. Tru Van Nguyen, Ms. Chathurika Dilhani, Ms. Sultan Pulat and Mr. Mücahit Varlı for the grate support and contribution during my PhD research.

I am deeply indebted to my beloved parents Yaşar and Memnune Taş, my dear brother Abdurrahman Yasin Taş, and my dear sister Yasemin Keydal and her lovely family Davut Keydal and Omer Arif Keydal (my little man) for their endless encouragement and support during my PhD.

Finally, I wish to express my deepest gratitude to my dear wife Hilal Taş for her endless encouragement, patience, and heartiest support for the past four and half years in Republic of Korea. I am also very grateful that I became father of honey baby Asel Taş who is miracle of my life.

Thank you very much all of you!